UC San Diego
UC San Diego Electronic Theses and Dissertations

Title

The M1-Fg Interaction and its Contribution to GAS Pathogenesis

Permalink

https://escholarship.org/uc/item/3619f9j6

Author

Stewart, Chelsea

Publication Date

2016

Peer reviewed|Thesis/dissertation

UNIVERSITY OF CALIFORNIA, SAN DIEGO

The M1-Fg Interaction and its Contribution to GAS Pathogenesis

A dissertation submitted in partial satisfaction of the requirements for the degree

Doctor of Philosophy

in

Biomedical Sciences

by

Chelsea Stewart

Committee in charge:

        Professor Partho Ghosh, Chair
        Professor Victor Nizet, Co-Chair
        Professor Tracy Handel
        Professor Sanford Shattil
        Professor Dong Wang

2016

The Dissertation of Chelsea Stewart is approved, and it is acceptable in quality and form for publication on microfilm and electronically:

_____

_____

_____

_____

Chair

University of California, San Diego

2016

DEDICATION

For my family

TABLE OF CONTENTS

LIST OF ABBREVIATIONS

µL. Microliter

CD. Circular dichroism

C-terminus. Carboxy-terminus

DNA. Deoxyribonucleic Acid

DTT. Dithiothreitol

E. coli. Escherichia coli

Fg. Fibrinogen

GAS. Group A Streptococcus

KCl. Potassium chloride

KP$_i$. Potassium phosphate

kDa. Kilodaltons

mg. milligram

mM. millimoles/liter

NaCl. Sodium chloride

NaF. Sodium fluoride

NaP$_i$. Sodium phosphate

NMR. Nuclear magnetic resonance

N-terminus. Amino-terminus

PAGE. Polyacrylamide gel electrophoresis

PBS. Phosphate buffered saline

PCR. Polymerase chain reaction

SDS. Sodium dodecyl sulfate

S. pyogenes. Streptococcus pyogenes

TBS. Tris-buffered saline

Tris. Tris Hydroxymethylaminoethane

WT. Wild type

LIST OF FIGURES

ACKNOWLEDGEMENTS

I would like to extend my deepest gratitude to Dr. Partho Ghosh for letting me explore the world of biochemistry and microbiology in his lab. He has been a supportive and patient mentor whose excitement for science is infectious. His advice has been invaluable in helping me approach science both during my time as a graduate student and on into the future. I will always appreciate the time and opportunity he has given me to grow as a researcher.

I would also like to thank Dr. Victor Nizet for being my co-chair and letting me use a bench in his lab. He always has a new perspective to offer and has inspired me to make extensions and keep the big picture in mind. I would also like to thank my committee, Dr. Tracy Handel, Dr. Sanford Shattil, and Dr. Dong Wang, for taking the time to provide me with feedback, help me grow as a researcher, and find the room in the depths of BSB I scheduled for my meeting.

Thank you also to everyone in the P. Ghosh lab, Dr. Brent Hamaoka, Dr. Andres Valderrama, Dr. Sumit Handa, Dr. Romila Mukerjea, and Cosmo Buffalo for sharing so many laughs and bring such liveliness to the lab. You all have provided such help over the years and have offered new perspectives to the projects happening in lab. Thank you also to the undergraduates Henry Quach and Clara Fu who brought such curiosity and joy to the lab and helped me grow as an educator.

Thank you also to all the members of the Nizet lab for putting up with me and helping me find pipet tips and the snack drawer. You are all so welcoming and

Chapter 2 in its entirety is pending publication as the Functional Significance for Coiled-coil Non-ideality in the Group A *Streptococcus* M1 Protein. Chelsea M. Stewart, Anna Henningham, Jason Cole, Andres Valderrama, Victor Nizet, Partho Ghosh. The dissertation author was the primary investigator and author of this work.

VITA

Education

2016   Ph.D., Biomedical Sciences
             University of California, San Diego

2009   B.S., Biochemistry
        B.S., Microbiology
             University of Washington, Seattle

ABSTRACT OF THE DISSERTATION

The M1-Fg Interaction and its Contribution to GAS Pathogenesis

by

Chelsea Stewart

Doctor of Philosophy in Biomedical Sciences

University of California, San Diego, 2016

Professor Partho Ghosh, Chair

The M protein is the major surface-associated virulence factor of Group A *Streptococcus* (GAS). M protein is predicted to be a parallel α-helical coiled coil, as identified by a heptad repeat pattern with small, hydrophobic residues at the first and fourth positions. To date, over 200 M variants have been identified, however a common trend among M proteins is that they contain regions characterized as non-ideal coiled coils, with both destabilizing residues in the putative dimer interface and skips and insertions in the heptad pattern. Crystallographic studies on M1 revealed

two distinct registers at the fibrinogen (Fg) binding sites: a Fg non-binding register 1 and a Fg-binding register 2. These conformations are related by a rotation of one helical face, resulting in the exposure of adjacent faces of the coiled coil. It was previously found that mutations stabilizing register 1 understandably reduced interaction with Fg. However, we now report that mutations stabilizing register 2 also reduce Fg binding. These results suggest that dynamic motion in M1 is required for association with Fg, in a "lure-and-catch" model. This requirement for binding offers a novel explanation for the presence of non-ideal coiled coil structure in M1, a feature that is evolutionarily conserved among M proteins in general.

The M1 protein contains three fibrinogen binding sites, one in the A region and two in the B repeats. Both binding sites in the B repeats are essential to establish a supramolecular complex capable of activating neutrophils. However the function of the binding site in the A region is still unknown. In addition to contributing to immune activation, the M1-fibrinogen interaction contributes to immune evasion. Surface recruitment of fibrinogen has been shown to protect against complement deposition and subsequent phagocytosis. We investigated the role of each fibrinogen binding site in conferring protection from phagocytosis.

Chapter 1

Introduction

The gram positive bacterial pathogen Group A *Streptococcus* (GAS) is one of the most prevalent pathogens in the world and is estimated to cause over 500,000 deaths a year (O'Loughlin et al., 2007). While found as a species that is commensal to the nose and throat, GAS can cause an array of diseases ranging from mild superficial infections to severe, invasive disease (Walker et al., 2014). Since the 1980's there has been an increase in the incidence of invasive disease due to GAS infection, suggesting the development of increased virulence (Aziz and Kotb, 2008). Despite the burden of disease from GAS, treatments are limited and there is no available vaccine, which is why a deeper understanding of the mechanisms of pathogenesis is necessary to direct novel treatments and support vaccine development.

BURDEN OF DISEASE

Group A *Streptococcus* is an exclusively human pathogen. Infection with GAS can result in superficial infections, severe, invasive disease, or post-infection sequelae. Superficial infections include pharyngitis and impetigo. While superficial infections of GAS have low mortality rates, they account for over 700 million cases annually (Carapetis et al., 2005). In contrast, severe, invasive disease resulting from infection with GAS accounts for only 660,000 cases annually but 160,000 deaths. Invasive diseases include bacteremia, streptococcal toxic shock syndrome (STSS), and necrotizing faciitis (Carapetis et al. 2005). Infections are generally treated with antibiotics, as GAS remains sensitive to penicillin. However, in some regions GAS is developing resistance to antibiotics such as macrolides, clindamycin, and lincosamide

(Hasenbein et al., 2004), so the emergence of a highly resistant strain is always a concern.

Infection with GAS has been linked to the development of associated sequelae, including post-streptococcal glomerulonephritis (470,000 new cases annually), the autoimmune disorder acute rheumatic fever (470,000 new cases annually), the further complication of rheumatic heart disease (282,000 new cases annually), and the newly described psychological disorder pediatric autoimmune neuropsychiatric disorders associated with streptococcal infections (PANDAS) (Kurlan et al., 2008). Acute rheumatic fever that leads to rheumatic heart disease accounts for over 233,000 deaths annually and is the leading cause of pediatric heart disease worldwide (Carapetis et al., 2005; Lee et al., 2009). The high rates of morbidity and mortality from rheumatic heart disease pose a great challenge for the development of a GAS vaccine against the surface virulence factor M protein, as antibodies generated exhibit crossreactivity to self proteins and is thus feared to potentially cause rheumatic heart disease (Cunningham and Quinn, 1997).

Epidemiological studies of GAS infection revealed a unique distribution of GAS serotypes. GAS is serotyped by the *emm* gene that encodes the surface-expressed M protein (Cunningham, 2000; Facklam et al., 1999; Todd and Lancefield, 1928). Currently there are over 200 different serotypes identified, some of which contain further genetic variation within the serotype. Isolates from invasive infections have been serotyped to numerous different M strains and is influenced by geographic location and year (Bessen, 2009; Carapetis et al., 2005). In industrialized countries, among the cases of invasive disease, over 20% are associated with the *emm*1 serotype,
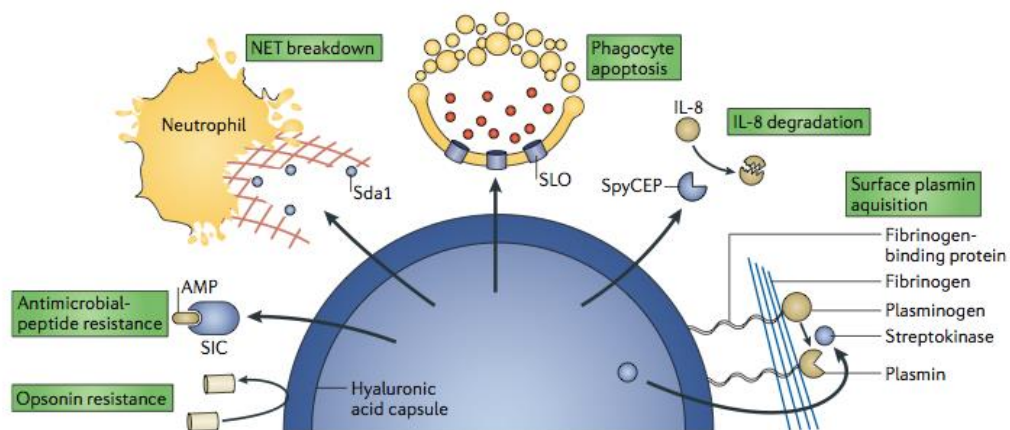
Figure 1.1 GAS Virulence Factors. Summary of virulence factors from GAS M1T1. Hyaluronic acid capsule and streptococcal inhibitor of complement (SIC) promote resistance to antimicrobial peptide (AMP); Extracellular streptodornase D (Sda1) degrades neutrophil extracellular traps (NETs); streptolysin O (SLO) causes apoptosis; interleukin-8 (IL-8) protease (SpyCEP) degrades IL-8; and M1 protein binds fibrinogen that recruits plasminogen. Adopted from Cole et al. (2011) *Nat. Rev. Microbiol.* 9, 724–36

making it the serotype with the highest incidence. However the *emm*1 serotype is among the most common isolates from asymptomatic carriers (Ekelund et al., 2005).

GAS PATHOGENESIS

GAS pathogenesis begins with adherence of bacteria to epithelial cells allowing for colonization. This process is initiated with the association of lipoteichoic acid to the host cell surface followed by tighter interaction through either lectin-carbohydrate or protein-protein interactions involving such bacterial factors as pili, M protein, hyaluronic acid capsule, and fibronectin-binding proteins (Nobbs et al., 2007). The factors involved in adherence to the cell surface can be strain specific and have been implicated in regulating tissue tropism. Following colonization, GAS utilize numerous factors to evade immune detection and promote infection. These factors include, but are not limited to, Sda1, a DNAse that degrades neutrophil extracellular traps; SLO, a cytolysin that triggers apoptosis in target cells; SpyCEP, a proteinase that cleaves chemokines; and IdeS, an IgG endopeptidase (Cole et al., 2011; Cunningham, 2000) (Fig. 1). The work in this thesis focuses on the M protein in particular and the mechanism by which M protein modulates immune response.

M PROTEIN

M protein is the major surface-expressed virulence factor of GAS and is encoded by the *emm* gene and is used to serotype GAS strains. M proteins all contain
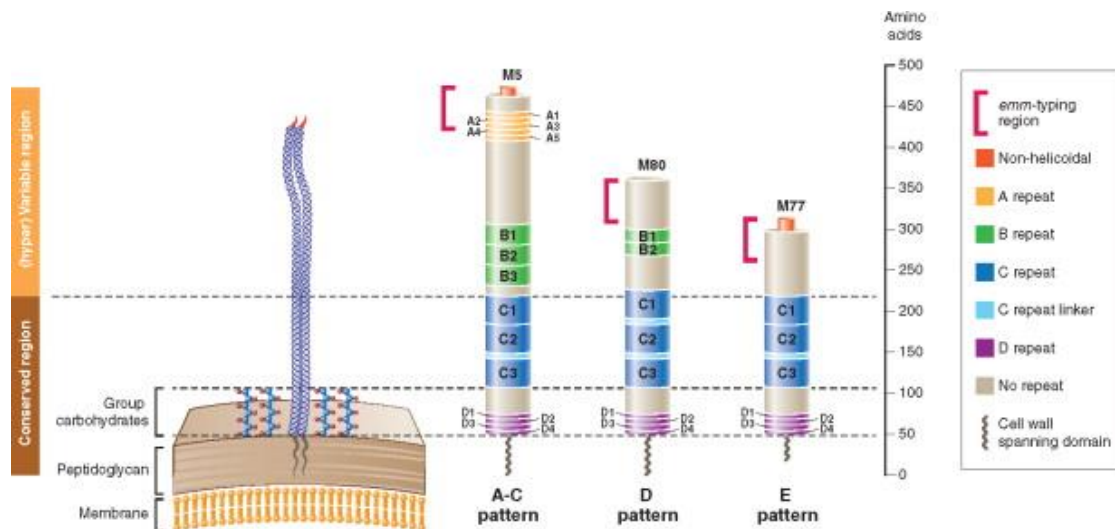
Figure 1.2 M Protein Patten Model. A representative M protein from each *emm* pattern type. Sequence conservation is high at the C-terminus and decreases towards the N-terminus. The N-terminal hypervariable region (HVR) is used to type GAS. M1 falls under the A-C pattern. Unlike M5 protein, M1 protein has an A region with no repeats and 2.2 B repeats. Pattern A-C strains are associated with throat infections, pattern D strains are associated with superficial skin infections, and pattern E strains are associated with both tissue types. Adopted from McMillan et al. (2013) *Clin. Microbiol. Infect.* 19, E222–9.

a conserved N-terminal signal sequence that is cleaved off prior to exposure on the surface (Fischetti, 1989). Following the signal sequence is the hypervariable region (HVR), the sequence used to type GAS strains. While the N terminal is highly variable, sequence conservation increases towards the C-terminus, with a conserved LPXTG motif used by Sortase A to anchor the M protein to the peptidoglycan layer (Schneewind et al., 1992) (Fig 2). M proteins are categorized into *emm* pattern groups based on location in the genome, pattern A-C, D or E, and then further subdivided into clusters based on sequence alignment. While all M proteins contain C repeats and D repeats at the C-terminus, the presence of A or B repeats varies depending on the pattern group or clade the M protein belongs to (McMillan et al., 2013; Sanderson-Smith et al., 2014).

M protein has been shown to be essential for full virulence in a mouse model of GAS infection and has been shown to be essential in multiple phases of pathogenesis (Ashbaugh et al., 1998). M protein has been implicated in host cell adhesion as well as host cell tropism (Bessen, 2009; Ellen and Gibbons, 1972). M protein also aids in immune evasion through binding host immune factors such as fibrinogen (Fg), complement inhibitory factor H, C4b-binding protein, and immunoglobulins (Fischetti, 1989). Binding of these factors to the bacterial surface effectively coats the bacterium, thereby preventing the deposition of complement factors and the opsonophagocytosis that would ensue (Carlsson et al., 2005). Additionally, M protein has been implicated in immune activation (Gautam et al., 2001). M protein has been shown to directly and indirectly recruit plasminogen to the
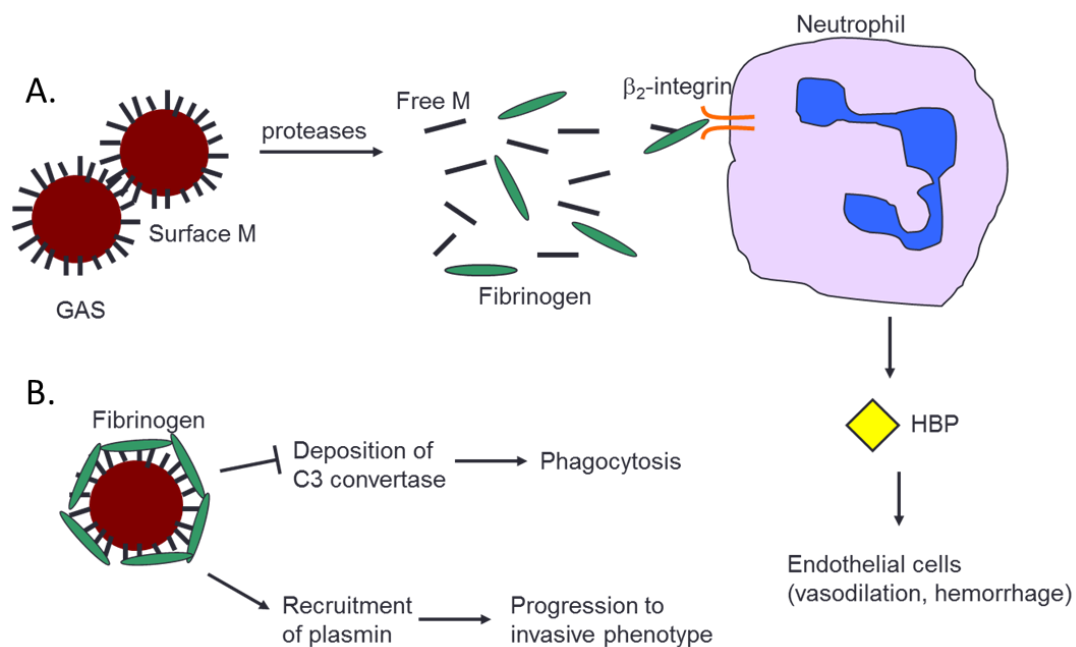
Figure 1.3 Model of the Immunological Response to the M1-Fg interaction. (A) Bacterial and neutrophil proteases cleave M1 protein and release it from the bacterial surface. Free M1 protein forms complexes with fibrinogen that activate neutrophils to release heparin binding protein (HBP). (B) Additionally, surface M1 protein can recruit fibrinogen that prevents the deposition of C3 convertase and the subsequent phagocytosis as well as recruits plasminogen that can be activated to plasmin.

bacterial surface, a step crucial to the transition to invasive disease (Cole et al., 2006; Sun et al., 2004). Moreover, bacterial and neutrophil proteases can cleave M protein to release it from the bacterial surface, resulting in free, soluble M1 protein that can interact with Fg to activate neutrophils (Fig. 3). Systemic injection of soluble M1 protein into a mouse was shown to be sufficient to trigger symptoms similar to STSS, notably vascular leakage and tissue injury (Herwald et al., 2004; McNamara et al., 2008; Soehnlein et al., 2008). Because it holds a prominent role in immune activation and immune evasion, the interaction of M protein with Fg is the focus of this work.

STRUCTURAL CHARACTERISTICS OF M PROTEIN

All M proteins are predicted to be parallel α-helical coiled coils that extend from the bacterial surface 30-90 nm (Fischetti, 1989; Manjula and Fischetti, 1980). Coiled coil proteins have a characteristic heptad repeat with small apolar residues at the first (*a*) and fourth (*d*) position of the repeat (Lupas et al., 1991; Woolfson and Alber, 1995). This pattern clusters the apolar residues into a hydrophobic face of the helix that facilitates oligomerization. For coiled coil dimers, the apolar residues pack in a knob-into-hole fashion to form the dimer interface (O'Shea et al., 1991) (Fig. 4). This process of dimerization is tolerant of sequence variation in the external positions, as long as the *a* and *d* positions are conserved (Tripet et al., 2000; Wagschal et al., 1999). However, heptad propensity analysis of M proteins revealed regions with a low likelihood of being in a coiled coil (Fig. 4). Additionally, sequence analysis of M1 and M5 proteins revealed atypical residues in predicted *a* and *d* positions, such as

A.

B.
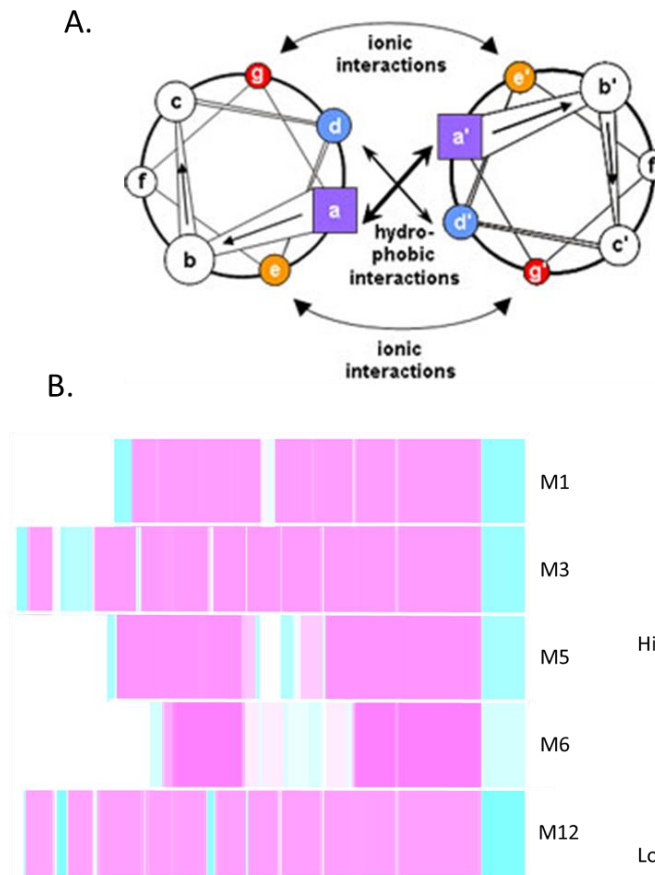
Figure 1.4 Dimeric Coiled Coil Pattern and Propensity. (A) Schematic of a helical wheel depicting the interactions of distinct heptad positions between subunits of a dimer. The *a* and *d* positions form knob-into-hole packing of hydrophobic residues while the *e* and *g* positions can contribute through ionic interactions. Adopted from Ghosh (2011) *Adv. Exp. Med. Biol.* 795: 197-211 (B) Heat map of coiled coil propensity of a selection of Fg-binding M proteins showing regions of low propensity for being a coiled coil. Propensity calculated from COILS (Lupas et al., 1991). This diagram does not include skips or insertions that may occur in the heptad pattern.

alanines and charged residues, and skips or insertions in the heptad pattern (McNamara et al., 2008; Nilson et al., 1995). Crystallographic studies of a fragment of the M1 protein revealed a non-ideal coiled coil structure with tightening of the helix caused by three Ala's at the dimer interface, then splaying of the helix caused by a Lys and Arg in the dimer interface, thereby confirming the predicted non-ideal nature of the coiled coil of M proteins (McNamara et al., 2008).

Interestingly, these aberrations from an ideal coiled coil structure also occur at the Fg binding site of M1 protein. Mature M1 protein contains five distinct regions: HVR, A region, B repeats, S region, C repeats, and D repeats. Fibrinogen binds the B repeats of M1 protein, a region composed of a 28 amino acid stretch that repeats 2.2 times, and is characterized by stretches of residues predicted to exist in two competing heptad registers (Macheboeuf et al., 2011). Interestingly, the co-crystal structure of an M1 fragment with Fg revealed a unique conformation of the B repeats compared to that of free M protein. This suggested two registers for the coiled coil at the B repeats, the free register (register 1) and the Fg-bound register (register 2), that are related by a rotation of one helical face. Despite these competing conformations, analysis with SOCKET (Walshaw and Woolfson, 2001), a program used to analyze knob-into-hole packing, reveals classic knob-into-hole packing across the Fg bound region of the coiled coil in register 2, raising the question of the role of register 1 and this span of non-ideal coiled coil residues.

Another intruiguing feature of the Fg-M1 interaction is that the binding site is located within a repeat, producing two Fg binding sites. An additional binding site was identified in the A region, establishing a total of three Fg binding sites for each
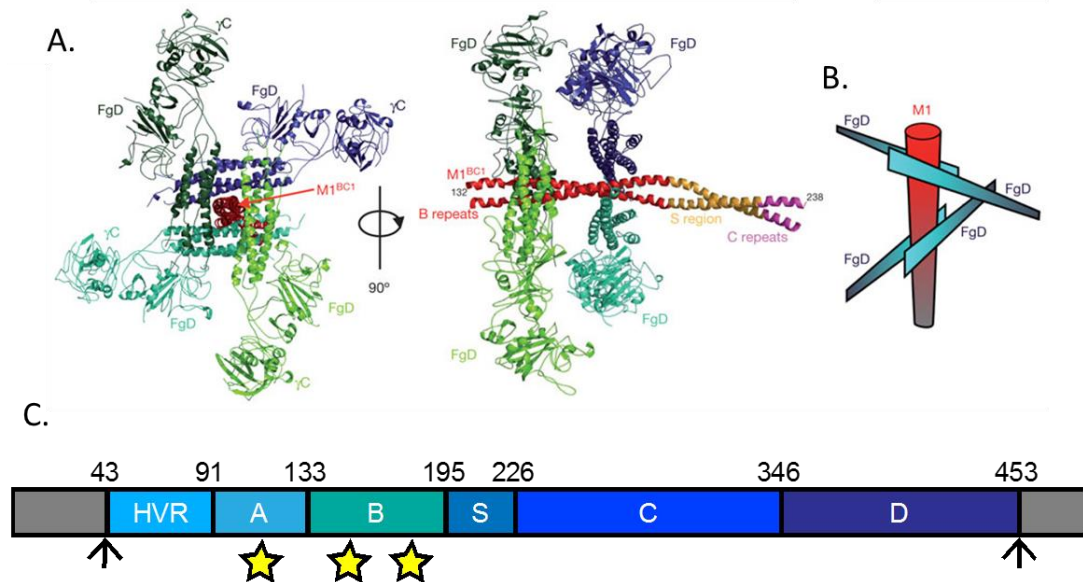
Figure 1.5 M1-Fg interaction. (A) Co-crystal structure of the B repeats of M1 protein and fibrinogen fragment D in a 2:4 ratio. Each Fg-binding site binds two molecules of Fg orientated 180° to one another. (B) Schematic of M1-FgD interaction showing the crosshatch structure that develops. Adopted from Macheboeuf et al. (2011) *Nature* 472: 64-68 (C) Diagram of M1 protein and its regions. Fibrinogen binding sites are indicated by stars, one in the A region and two in the B repeats. Arrows indicate signal sequence cleavage sites.

M1 molecule. Each Fg binding site binds two molecules of Fg ~180° to each other for a total binding ratio of 2:6 (Fig. 5). Studies on free M1 protein and immune activation determined both sites in the B repeats to be essential for function (Macheboeuf et al., 2011). Surface bound Fg has been implicated in protecting from phagocytosis, however the binding requirements have not been defined and the function of the third binding site in the A region is still unknown.

RESEARCH GOALS

The work presented here investigates these unique structural features of the Fg binding sites of M1 protein. Chapter 2 presents on the non-ideal coiled coil nature of the Fg binding sites. It addresses the question of the role of structural dynamics and of each unique register through assaying mutants idealized into one register or the other. Chapter 3 focuses on the role of the multiplicity of binding sites within M1 protein. Binding requirements for phagocytosis protection was studied using GASΔemm complemented with constructs of M1 protein containing deletions in one or multiple Fg-binding sites. These studies further illuminate the mechanistic requirements of the M protein- Fg interaction necessary for pathogenesis.

REFERENCES

Ashbaugh, C.D., Warren, H.B., Carey, V.J., Wessels, M.R., 1998. Molecular analysis of the role of the group A streptococcal cysteine protease, hyaluronic acid capsule, and

M protein in a murine model of human invasive soft-tissue infection. J. Clin. Invest. 102, 550–60.

Aziz, R.K., Kotb, M., 2008. Rise and persistence of global M1T1 clone of Streptococcus pyogenes. Emerging Infect. Dis. 14, 1511–7.

Bessen, D.E., 2009. Population biology of the human restricted pathogen, Streptococcus pyogenes. Infect. Genet. Evol. 9, 581–93.

Carapetis, J.R., Steer, A.C., Mulholland, E.K., Weber, M., 2005. The global burden of group A streptococcal diseases. Lancet Infect Dis 5, 685–94.

Carlsson, F., Sandin, C., Lindahl, G., 2005. Human fibrinogen bound to Streptococcus pyogenes M protein inhibits complement deposition via the classical pathway. Mol. Microbiol. 56, 28–39.

Cole, J.N., Barnett, T.C., Nizet, V., Walker, M.J., 2011. Molecular insight into invasive group A streptococcal disease. Nat. Rev. Microbiol. 9, 724–36.

Cole, J.N., McArthur, J.D., McKay, F.C., Sanderson-Smith, M.L., Cork, A.J., Ranson, M., Rohde, M., Itzek, A., Sun, H., Ginsburg, D., Kotb, M., Nizet, V., Chhatwal, G.S., Walker, M.J., 2006. Trigger for group A streptococcal M1T1 invasive disease. FASEB J. 20, 1745–7.

Cunningham, M.W., 2000. Pathogenesis of group A streptococcal infections. Clin. Microbiol. Rev. 13, 470–511.

Cunningham, M.W., Quinn, A., 1997. Immunological crossreactivity between the class I epitope of streptococcal M protein and myosin. Adv. Exp. Med. Biol. 418, 887–92.

Ekelund, K., Skinhøj, P., Madsen, J., Konradsen, H.B., 2005. Reemergence of emm1 and a changed superantigen profile for group A streptococci causing invasive infections: results from a nationwide study. J. Clin. Microbiol. 43, 1789–96.

Ellen, R.P., Gibbons, R.J., 1972. M protein-associated adherence of Streptococcus pyogenes to epithelial surfaces: prerequisite for virulence. Infect. Immun. 5, 826–30.

Facklam, R., Beall, B., Efstratiou, A., Fischetti, V., Johnson, D., Kaplan, E., Kriz, P., Lovgren, M., Martin, D., Schwartz, B., Totolian, A., Bessen, D., Hollingshead, S., Rubin, F., Scott, J., Tyrrell, G., 1999. emm typing and validation of provisional M types for group A streptococci. Emerging Infect. Dis. 5, 247–53.

Fischetti, V.A., 1989. Streptococcal M protein: molecular design and biological behavior. Clin. Microbiol. Rev. 2, 285–314.

Gautam, N., Olofsson, A.M., Herwald, H., Iversen, L.F., Lundgren-Akerlund, E., Hedqvist, P., Arfors, K.E., Flodgaard, H., Lindbom, L., 2001. Heparin-binding protein (HBP/CAP37): a missing link in neutrophil-evoked alteration of vascular permeability. Nat. Med. 7, 1123–7.

Hasenbein, M.E., Warner, J.E., Lambert, K.G., Cole, S.E., Onderdonk, A.B., McAdam, A.J., 2004. Detection of multiple macrolide- and lincosamide-resistant strains of Streptococcus pyogenes from patients in the Boston area. J. Clin. Microbiol. 42, 1559–63.

Herwald, H., Cramer, H., Mörgelin, M., Russell, W., Sollenberg, U., Norrby-Teglund, A., Flodgaard, H., Lindbom, L., Björck, L., 2004. M protein, a classical bacterial virulence determinant, forms complexes with fibrinogen that induce vascular leakage. Cell 116, 367–79.

Kurlan, R., Johnson, D., Kaplan, E.L., 2008. Streptococcal infection and exacerbations of childhood tics and obsessive-compulsive symptoms: a prospective blinded cohort study. Pediatrics 121, 1188–97.

Lee, J.L., Naguwa, S.M., Cheema, G.S., Gershwin, M.E., 2009. Acute rheumatic fever and its consequences: a persistent threat to developing nations in the 21st century. Autoimmun Rev 9, 117–23.

Lupas, A., Dyke, M. Van, Stock, J., 1991. Predicting coiled coils from protein sequences. Science 252, 1162–4.

Macheboeuf, P., Buffalo, C., Fu, C., Zinkernagel, A., Cole, J., Johnson, J., Nizet, V., Ghosh, P., 2011. Streptococcal M1 protein constructs a pathological host fibrinogen network. Nature 472, 64–8.

Manjula, B.N., Fischetti, V.A., 1980. Tropomyosin-like seven residue periodicity in three immunologically distinct streptococal M proteins and its implications for the antiphagocytic property of the molecule. J. Exp. Med. 151, 695–708.

McMillan, Drèze, -A., Vu, Bessen, Guglielmini, Steer, Carapetis, Melderen, Sriprakash, Smeesters, 2013. Updated model of group A Streptococcus M proteins based on a comprehensive worldwide study. Clin. Microbiol. Infect. 19, E222–9.

McNamara, C., Zinkernagel, A., Macheboeuf, P., Cunningham, M., Nizet, V., Ghosh, P., 2008. Coiled-coil irregularities and instabilities in group A Streptococcus M1 are required for virulence. Science (New York, N.Y.) 319, 1405–8.

Nilson, B., Frick, I.-M., Aakesson, P., Forsen, S., Bjoerck, L., Aakerstroem, B., Wikstroem, M., 1995. Structure and Stability of Protein H and the M1 Protein from

Streptococcus pyogenes. Implications for Other Surface Proteins of Gram-Positive Bacteria. Biochemistry 34, 1368813698.

Nobbs, A.H., Shearer, B.H., Drobni, M., Jepson, M.A., Jenkinson, H.F., 2007. Adherence and internalization of Streptococcus gordonii by epithelial cells involves beta1 integrin recognition by SspA and SspB (antigen I/II family) polypeptides. Cell. Microbiol. 9, 65–83.

O'Loughlin, R.E., Roberson, A., Cieslak, P.R., Lynfield, R., Gershman, K., Craig, A., Albanese, B.A., Farley, M.M., Barrett, N.L., Spina, N.L., Beall, B., Harrison, L.H., Reingold, A., Beneden, C. Van, 2007. The epidemiology of invasive group A streptococcal infection and potential vaccine implications: United States, 2000-2004. Clin. Infect. Dis. 45, 853–62.

O'Shea, E.K., Klemm, J.D., Kim, P.S., Alber, T., 1991. X-ray structure of the GCN4 leucine zipper, a two-stranded, parallel coiled coil. Science 254, 539–44.

Sanderson-Smith, M., Oliveira, D.M. De, Guglielmini, J., McMillan, D.J., Vu, T., Holien, J.K., Henningham, A., Steer, A.C., Bessen, D.E., Dale, J.B., Curtis, N., Beall, B.W., Walker, M.J., Parker, M.W., Carapetis, J.R., Melderen, L. Van, Sriprakash, K.S., Smeesters, P.R., 2014. A systematic and functional classification of Streptococcus pyogenes that serves as a new tool for molecular typing and vaccine development. J. Infect. Dis. 210, 1325–38.

Schneewind, O., Model, P., Fischetti, V.A., 1992. Sorting of protein A to the staphylococcal cell wall. Cell 70, 267–81.

Soehnlein, Oehmcke, X, Rothfuchs, Frithiof, van Rooijen, Mörgelin, Herwald, Lindbom, 2008. Neutrophil degranulation mediates severe lung damage triggered by streptococcal M1 protein. European Respiratory Journal 32, 405–12.

Sun, H., Ringdahl, U., Homeister, J.W., Fay, W.P., Engleberg, N.C., Yang, A.Y., Rozek, L.S., Wang, X., Sjöbring, U., Ginsburg, D., 2004. Plasminogen is a critical host pathogenicity factor for group A streptococcal infection. Science 305, 1283–6.

Todd, E.W., Lancefield, R.C., 1928. VARIANTS OF HEMOLYTIC STREPTOCOCCI; THEIR RELATION TO TYPE-SPECIFIC SUBSTANCE, VIRULENCE, AND TOXIN. J. Exp. Med. 48, 751–67.

Tripet, B., Wagschal, K., Lavigne, P., Mant, C.T., Hodges, R.S., 2000. Effects of side-chain characteristics on stability and oligomerization state of a de novo-designed model coiled-coil: 20 amino acid substitutions in position "d". J. Mol. Biol. 300, 377–402.

Wagschal, K., Tripet, B., Lavigne, P., Mant, C., Hodges, R.S., 1999. The role of position a in determining the stability and oligomerization state of alpha-helical coiled coils: 20 amino acid stability coefficients in the hydrophobic core of proteins. Protein Sci. 8, 2312–29.

Walker, M.J., Barnett, T.C., McArthur, J.D., Cole, J.N., Gillen, C.M., Henningham, A., Sriprakash, K.S., Sanderson-Smith, M.L., Nizet, V., 2014. Disease manifestations and pathogenic mechanisms of group a Streptococcus. Clin. Microbiol. Rev. 27, 264–301.

Walshaw, J., Woolfson, D.N., 2001. Socket: a program for identifying and analysing coiled-coil motifs within protein structures. J. Mol. Biol. 307, 1427–50.

Woolfson, D.N., Alber, T., 1995. Predicting oligomerization states of coiled coils. Protein Sci. 4, 1596–607.

Chapter 2

Structural Dynamics of the Non-ideal Coiled Coil Region of M1 Protein are Essential for Binding Fibrinogen

INTRODUCTION

The antigenically variable M protein is the major surface-associated virulence factor of Group A *Streptococcus* and has a role in each of the diverse diseases manifested by this widespread bacterial pathogen (Cole et al., 2011; Cunningham, 2000; Hirst and Lancefield, 1939; Todd and Lancefield, 1928; Walker et al., 2014). While over 200 variants of the M protein have been identified (M1, M2, etc.), they are all predicted to form dimeric α-helical coiled coils (Fischetti, 1989; Phillips et al., 1981). This prediction is based primarily on the presence of heptad sequence repeats. Heptad repeats, which are diagnostic of coiled coils, are characterized by small, hydrophobic residues occupying the *a* and *d* positions of the [*abcdefg*]$_n$ heptad. The small, hydrophobic residues in the *a* position from each helix engage in 'knobs-into-hole' packing with each other, as do the residues in the *d* position, thereby forming the hydrophobic core of the dimer (Fig. 2.1b) (Crick 1953). In dimeric coiled coils, Val and Leu are preferred at the *a* and *d* positions, respectively (Lupas et al., 1991; Tripet et al., 2000; Wagschal et al., 1999; Woolfson and Alber, 1995).

Curiously, M proteins diverge from this ideal pattern. M proteins have an unusually high proportion of coiled-coil destabilizing residues (e.g., charged residues occupying predicted *a* and *d* positions) and disruptions in their heptad patterns (i.e., short insertions or deletions) (Macheboeuf et al., 2011; McNamara et al., 2008; Nilson et al., 1995). The effects of such disturbances have been visualized in the structure of an M1 protein fragment, in which Lys 98 and Arg 105 at successive *a*
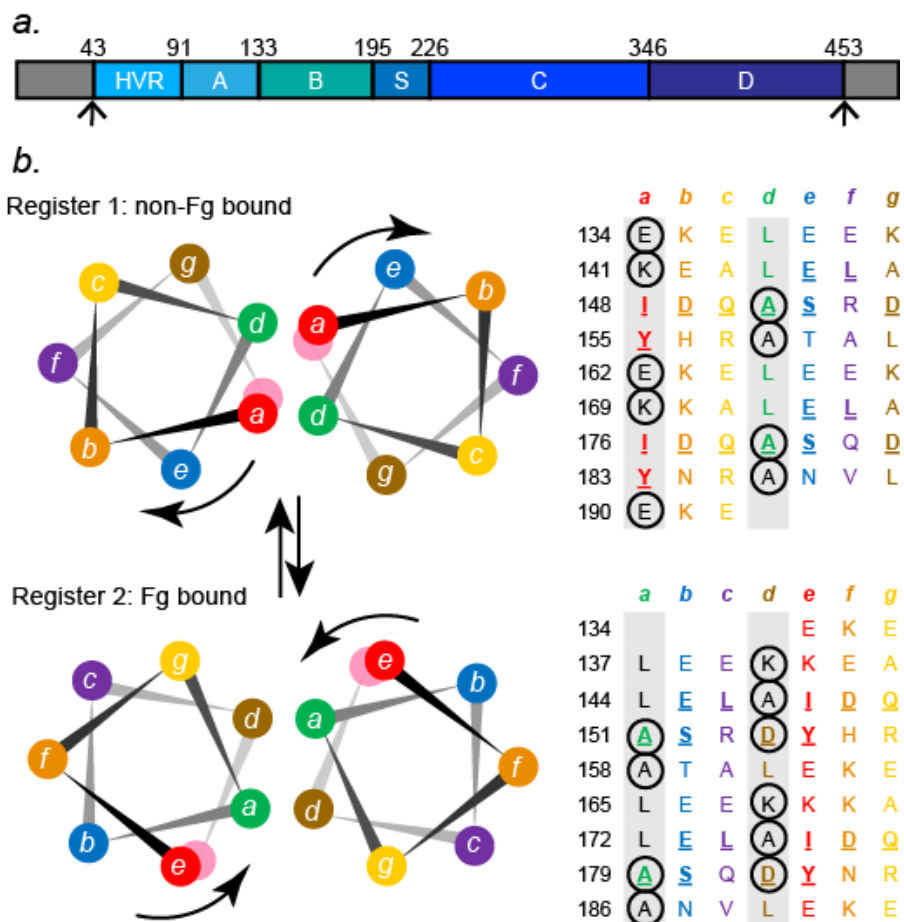
Figure 2.1. M1 is a non-ideal coiled coil. (a) Schematic of the M1 protein. Arrows indicate signal cleavage sites. (b)Helical wheel and heptad repeat schematic of the two registers of the B repeats of M1 protein, register 1 (free M1 crystal structure) and register 2 (the M1-Fg cocrystal structure). The heptad positions, *a* and *d*, that compose the dimer interface are indicated in grey for each register. Residues observed to bind Fg in register 2 are underlined; the same residues are underlined in register 1. To generate M1*[1R] and M1*[2R], the residues in black were mutated to valines (*a* position) or leucines (*d* position) in register 1 and 2, respectively. Destabilizing residues in the dimer interface are circled.

positions were seen to cause unwinding of the coiled coil (McNamara et al., 2008).

The high proportion of coiled-coil destabilizing residues is consistent with the perplexing loss of structure at physiological temperature (McNamara et al., 2008;

Nilson et al., 1995). Why loss of structure in M proteins is conducive to *in vivo* function is unexplained. We sought to understand why non-ideal heptad patterns are prevalent in M proteins.

To address this issue, we used the functionally and structurally characterized B repeats of the M1 protein (Fig. 2.1b). The M1 B repeats confer binding to human fibrinogen (Fg), an interaction key to phagocytic resistance and proinflammatory activation seen during septic shock (Herwald et al., 2004; Macheboeuf et al., 2011; Uchiyama et al., 2013). These repeats are composed of two 28-residue regions that differ slightly in sequence but are completely conserved in the residues that interact with Fg. Notably, the B repeats have been observed to have different heptad registers depending on whether they are free (register 1) or Fg-bound (register 2). The two registers are related to one another by a rotation of one helical face, and present a different set of exposed residues for interaction (Fig. 2.1b) (Macheboeuf et al., 2011). Coiled-coil destabilizing residues occur with near equal frequency in registers 1 and 2. Indeed, the prevalence of destabilizing residues is high enough that sequence analysis suggests that the B repeats are composed of short segments of register 1-preferring residues interspersed with short segments of register 2-preferring residues (Fig. 2.2b).

To understand the significance of coiled-coil destabilizing residues, we idealized the B repeats to promote the formation of a stable coiled-coil. Idealization

a.

b.

	a	b	c	d	e	f	g
134					E	K	E
137	L	E	E	K	K	E	A
144	L	E				L	A
148	I	D	Q	A	S	R	D
155	Y					H	R
158	A	T	A	L	E	K	E
165	L	E	E	K	K	K	A
172	L	E				L	A
176	I	D	Q	A	S	Q	D
183	Y					N	R
186	A	N	V	L	E	K	E

c.

M1*1R

	a	b	c	d	e	f	g
134	V	K	E	L	E	E	K
141	V	E	A	L	E	L	A
148	!	D	Q	A	S	R	D
155	Y	H	R	L	T	A	L
162	V	K	E	L	E	E	K
169	V	K	A	L	E	L	A
176	!	D	Q	A	S	Q	D
183	Y	N	R	L	N	V	L
190	V	K	E				

M1*2R

	a	b	c	d	e	f	g
134					E	K	E
137	V	E	E	L	K	E	A
144	V	E	L	L	!	D	Q
151	A	S	R	D	Y	H	R
158	V	T	A	L	E	K	E
165	V	E	E	L	K	K	A
172	V	E	L	L	!	D	Q
179	A	S	Q	D	Y	N	R
186	V	N	V	L	E	K	E
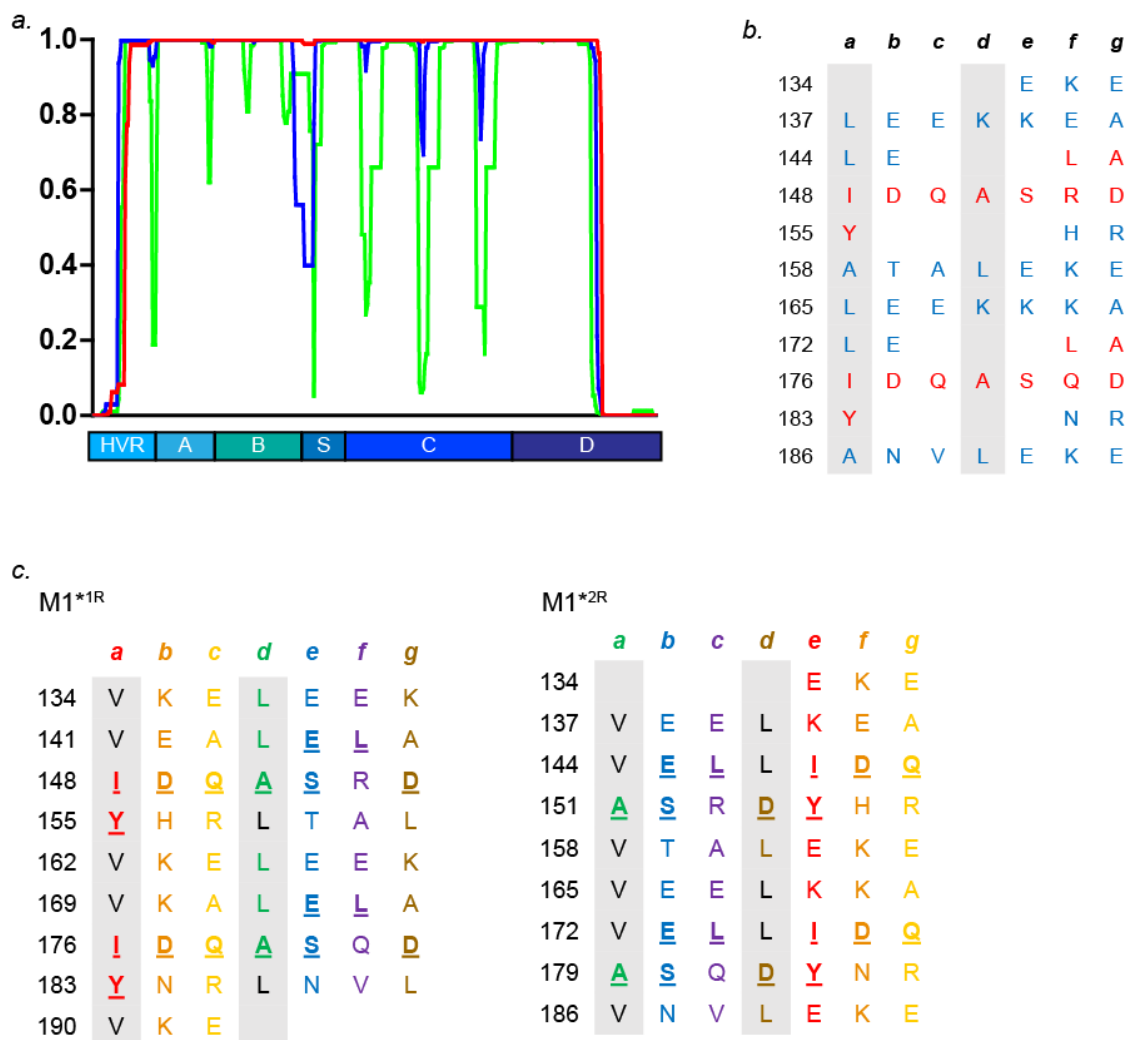
Figure 2.2. Non-ideal nature of the B repeats. (a) Coiled coil propensity predicted from COILS in a 14- (green), 21- (blue), or 28- (red) residue window. Schematic of M protein is below to reference where these breaks in coiled coil occur. (b) Predicted heptad positions of residues in the B repeats. Residues that align to register 1 are in blue, those that align to register 2 are in red, and those that contact fibrinogen are underlined. (c) Sequence of M1*1R and M1*2R highlighting the idealizing mutations made in black.

involved the substitution of residues in the *a* position with Val and in the *d* position with Leu. These substitutions were made in register 1 (M1*^{1R}) and separately in register 2 (M1*^{2R}), while maintaining the Fg-contacting residues (Fig. 2.2c). That is, the resulting M1 protein variants continue to contain all the residues seen to contact Fg (when M protein is in register 2). Prior work had shown that M1*^{1R} was attenuated in Fg-binding (Mcnamara et al., 2008; Uchiyama et al., 2013), as would be expected for stabilization in the Fg-nonbinding register. We now report the surprising result that stabilization in register 2 leads to an equal deficiency in Fg-binding. This result indicates that structural stability is inimical to specific interaction with Fg, and that dynamics in the coiled coil, as brought about by coiled-coil destabilizing residues, are necessary for this interaction. Furthermore, this results suggests that destabilizing residues are maintained in M proteins in general to permit functional protein-protein interactions necessary for pathogenesis.

MATERIALS AND METHODS

CLONING AND DNA MANIPULATION

The coding sequence for mature M1 protein (residues 42-453) and the AB fragment (residues 42-194) were cloned from the GAS strain 5448 into pET28b. The constructs included an N-terminal His$_6$-tag followed by a PreScission protease cleavage site or a C-terminal His$_6$-tag. Single-site substitutions were introduced by QuikChange (Stratagene). Idealization of the B repeats in register 2 was achieved by synthesizing a DNA fragment in which the *a* position residues L137, L144, A158,

L165, L172, and A186 were substituted with valine and the *d* position residues K140, A147, K168, and A175 with leucine. This DNA fragment was incorporated into the coding sequence for mature M1 protein as described previously (Mcnamara et al., 2008).

EXPRESSION AND PURIFICATION

Proteins were expressed in *E. coli* BL21 (DE3) Gold (Agilent). Bacteria were grown with shaking in LB media at 37 °C to mid-log phase and induced with 1 mM isopropyl-β-D-thiogalactopyranoside (IPTG). Following induction, bacteria were grown at 22 °C for 18 h with shaking and harvested by centrifugation (2000 x *g*, 30 min, 4 °C). Bacterial pellets were resuspended in lysis buffer (300 mM NaCl, 100 mM NaP$_i$, pH 7.5, 0.5 mM phenylmethanesulfonyl fluoride; 20 mL per L of initial bacterial culture) containing 200 µg/mL lysozyme and 100 µg/mL DNase, and lysed using an EmulsiFlex-C5 (Avestin; 20,000 psi with three passes). Lysates were clarified by centrifugation (35,000 x *g*, 45 min, 4 °C), filtered through a 0.22 µm membrane (Milipore), and added to a Ni^{2+}-NTA agarose column (RT, 5 mL resin per L of initial bacterial culture; Sigma) that had been pre-equilibrated with lysis buffer. The column was washed with 50 column volumes of wash buffer (500 mM NaCl, 50 mM NaP$_i$, pH 7.5, 20 mM imidazole) and eluted with three column volumes of elution buffer (300 mM NaCl, 100 mM NaP$_i$, pH 7.5, 500 mM imidazole). Purified proteins were dialyzed against 2 L of buffer A (75 mM NaCl, 20 mM NaP$_i$, pH 7.5) at 4 °C overnight (3500 MWCO tubing, Spectrum Laboratories). In cases in which the His$_6$-tag was removed, eluates were incubated with PreScission Protease (0.5 mg per 2 L initial bacterial

culture) and 5 mM DTT added directly to the dialysis tubing. Samples incubated with PreScission protease were further purified by Ni^{2+}-NTA chromatography, as described above, except that the flow-through was collected. Finally, proteins were concentrated to 2-17 mg/mL by ultrafiltration (3500 MWCO membrane, Amicon), aliquoted, and flash frozen in liquid N_2 for storage at -80 °C.

CYSTEINE PROBES

Monomeric forms of Cys substitution mutants of M1, AB*[1R], and AB*[2R] were prepared by diluting these proteins to 0.5 mg/mL in buffer A containing 100 mM DTT, and the samples were then heated at 60 °C for 3 h. Samples were then diluted 1:10 to 1:100 in buffer A and incubated at RT for 3 h. Prior to analysis, iodoacetamide was added to a concentration of 50 mM and the sample was incubated at RT for 15 min. Samples were then resolved by SDS-PAGE and visualized by Coomassie staining or Western blot. For the Western blot, samples were transferred from the polyacrylamide gel to a polyvinylidene fluoride membrane (Millipore) at 100 V for 40 min. Membranes were incubated in TBS (150 mM NaCl, 50 mM Tris, pH 8.0) for 10 min, and then blocked with 5% nonfat milk in TBS for 30 min. Membranes were incubated in TBS containing 5% nonfat milk, 0.05% Tween-20, and mouse horseradish peroxidase (HRP)-conjugated anti-His tag monoclonal antibody (1:2000, Santa Cruz Biotechnologies 8036) or rabbit anti-M1 protein polyclonal antibody (1:500) at 4 °C overnight. Membranes were then washed three times in TBS containing 0.05% Tween-20 for 15 min each. Membranes incubated with anti-M1 protein antibodies were then incubated in TBS containing 5% nonfat milk, 0.05%

Tween-20, and HRP-conjugated goat anti-rabbit IgG (1:5000, Santa Cruz Biotechnologies 2004) for 30 min at RT and washed as described above. SuperSignal West chemiluminescent substrate (Thermo Fisher Scientific) was used for detection, according to the manufacturer's instructions.

CIRCULAR DICHROISM SPECTROSCOPY

CD spectra were collected between 195 and 260 nm at 4 °C with 1 nm intervals and between 4 °C and 95 °C at 222 nm with 1° intervals using a quartz cell with a 1 cm pathlength on a model 202 spectrometer (Aviv Instruments) equipped with thermoelectric temperature control. For AB fragments, measurements were collected on samples at 9.8-12.2 μM, as determined by absorption using a calculated absorption coefficient, in 40 mM NaF, 10 mM NaPi, pH 7.5. For intact M1, measurements were collected on samples at 3.6-5.7 μM in 40 mM NaF, 20 mM NaPi, pH 7.5. The CD signal from buffer alone was subtracted from the data prior to conversion to mean residue ellipticity.

NUCLEAR MAGNETIC RESONANCE SPECTROSCOPY

AB and AB*^{2R} were grown and expressed in minimal media supplemented with $^{15}NH_4Cl$ (Cambridge Isotopes), and purified as described above. Purified protein at 3 mg/mL was dialyzed against 2 L of 75 mM NaCl, 20 mM Tris, pH 7.5, as described above and supplemented with 10% D_2O. NMR experiments were recorded at 26 °C on Varian VNMRS 800MHz spectrometer, equipped with a 5mm triple-

resonance coldprobe. 2D 1H-15N HSQC were recorded using standard pulse sequence included in the Varian BioPack. Data were processed using NMRPipe software.

FIBRINOGEN AND IgG Fc BINDING ASSAY

Fifty µL of His$_6$-tagged M1 and AB constructs at a concentration of 20 µM were incubated for 1 h at 37 °C under rotation with 50 µL Ni^{2+}-NTA agarose beads that had been pre-equilibrated with buffer A. The sample was centrifuged (500 x g, RT, 1 min) and the supernatant was removed. Fifty µL of either 20 µM fibrinogen fragment D (Calbiochem 341578), prepared as described previously (Everse 1995), or 40 µM IgG F$_c$ (Calbiochem 401104) in buffer A was added to the resin and incubated for 1 h at 37 °C with rotation. The sample was centrifuged (500 x g, RT, 1 min) and the supernatant was collected as the unbound fraction. The resin was washed with 1 mL of buffer A containing 20 mM imidazole and then centrifuged (500 x g, RT, 1 min), after which the supernatant was removed. This washing step was repeated three times, and proteins bound to the resin were then eluted with 30 µL buffer A containing 500 mM imidazole. The unbound fraction and elution samples were resolved and visualized by Coomassie-stained SDS-PAGE.

HEPARIN BINDING PROTEIN RELEASE ASSAY

One hundred microliters of human blood collected from healthy donors was diluted in PBS to a final volume of 1.0 mL and incubated with 2 µM M proteins for 45 minutes. Cells were centrifuged (300 x g, RT15 min) and the resulting supernatants were analyzed for HBP by sandwich ELISA following the manufacturer's instructions

(MyBiosouce.com Human Heparin Binding Protein ELISA kit Catalog # MBS029367).

COMPLEMENTED STRAINS: EXPRESSION AND FIBRINOGEN BINDING ASSAY

Genes encoding M1*^{1R} and M1*^{2R} were cloned into pDCErm and transformed into electrocompetent *S. pyogenes* (*Δemm1*) bacteria as previously described (Lauth et al., 2009). *S. pyogenes* was grown in stationary culture at 37 °C to mid-log phase and harvested by centrifugation (3000 x *g*, 15 min, 4 °C). Bacterial pellets were resuspended in PBS containing 100 µg/mL FgD and incubated with end-over-end rotation at 37 °C for 1 hr. Bacteria were pelleted by centrifugation (3000 x *g*, 15 min, 4 °C), washed in 1 mL PBS three times, then resuspended in 40% sucrose, 100 mM KP$_i$, pH 6.2, 10 mM MgCl$_2$, 2 mg/mL lysozyme, 500 U/mL mutanolysin, and incubated with rotation at 37 °C for 1 hr. The soluble cell wall fraction was collected after centrifugation (13,000 x *g*, 10 min, RT) and resolved by SDS-PAGE. M1 protein and fibrinogen were detected through Western blot as described above or with mouse monoclonal anti-fibrinogen γ (1:1000 Santa Cruz Biotechnologies 133156) and HRP-conjugated goat anti-mouse IgG (1:5000 Santa Cruz Biotechnologies 2005) antibodies. Bacterial surface expression of M protein and surface binding of Fg was assayed through flow cytometry. For this, overnight growths of *S. pyogenes* were diluted into 10 mL THB and grown to mid-log phase. Cultures were pelleted by centrifugation (3000 x *g*, 10 min, 20 °C) and washed with 5 mL PBS containing 0.1% BSA. Bacteria were resuspended in PBS and incubated with either anti-M1 antibody or naïve serum (1:1000, 60 min, 4 °C), or 10 µg/ml FITC-labeled Fg generated with

the Fluoreporter kit (Life Technologies). Bacteria were pelleted (3000 x *g*, 10 min, 20 °C) and washed twice with PBS containing 0.1% BSA. Samples probing for M1 were then incubated with the secondary antibody Alexa-488 anti-mouse IgG (1:500, 60 min, 4 °C, Life Technologies #A11001). Samples were pelleted by centrifugation (3000 x *g*, 10 min, 20 °C) and washed as above. Following the last wash, all samples were resuspended in PBS and analyzed by flow cytometry using a FACS Canto.

RESULTS

IDEALIZING THE COILED COIL RESTRICTS THE B REPEATS TO THE INTENDED CONFORMATION

We began our studies by verifying that register 1- and 2-idealizing substitutions had resulted in molecules that adopted those particular respective registers. We turned to the AB fragment of the M1 protein for this study, as this fragment is more unstable than intact M1 protein and thus provides a more stringent test of the mutations. The AB fragment contains the A region and B repeats of mature M1 but lacks the S region, C repeats, and D region (Fig. 2.1a). An M1 protein fragment approximating the AB fragment has been shown to be generated physiologically during conditions mimicking infection (Berge and Björck, 1995; Herwald et al., 2004). To assess which register the AB fragment idealized in register 1 (AB*[1R]) and in register 2 (AB*[2R]) assumed, we constructed cysteine substitutions as conformational probes. M1 protein itself contains no native cysteines. We surmised that the substituted cysteines would form intra-dimer disulfides if they occupied the *a*

or *d* position, but not if they occupied other heptad positions. The E162C substitution was created as a probe for register 1, as this residue occupies the core *a* heptad position in register 1 but the exterior *e* heptad position in register 2 (Fig. 2.1b). The L161C substitution was created as a probe for register 2, as this residue occupies the core *d* position in register 2 but the exterior *g* heptad position in register 1. Lastly, the A160C substitution mutant was created as a negative control, as it occupies exterior heptad positions in both registers (*f* in register 1, *c* in register 2) and thus should not be capable of forming intra-dimer disulfides.

For the Cys probe experiments, we first fully reduced AB*^{1R} and AB*^{2R} containing each of the three Cys substitutions (Fig. 2.3a, b Left). This was done to avoid confounding inter-dimer disulfides that might form during expression or purification, and was achieved by heating the proteins to cause dissociation and incubating them with 100 mM DTT. The samples were then cooled and diluted in the absence of DTT to enable reassociation into dimers and the formation of intra-dimer disulfides. Prior to denaturation and analysis by non-reducing SDS-PAGE, the samples were treated with iodoacetamide so as to block any remaining free cysteines that might yield artifactual disulfide bonds. This set of experiments showed that disulfide-linked dimers formed for E162C, the probe for register 1, only in the case of AB*^{1R} (Fig. 2.3a). Likewise, disulfide-linked dimers formed for L161C, the probe for register 2, only in the case AB*^{2R} (Fig. 2.3b). No disulfide-linked dimers were observed for A160C in either AB*^{1R} or AB*^{2R}, confirming that the disulfides observed for E162C and L161C were indeed intra-dimer (Fig. 2.3). These results indicate that
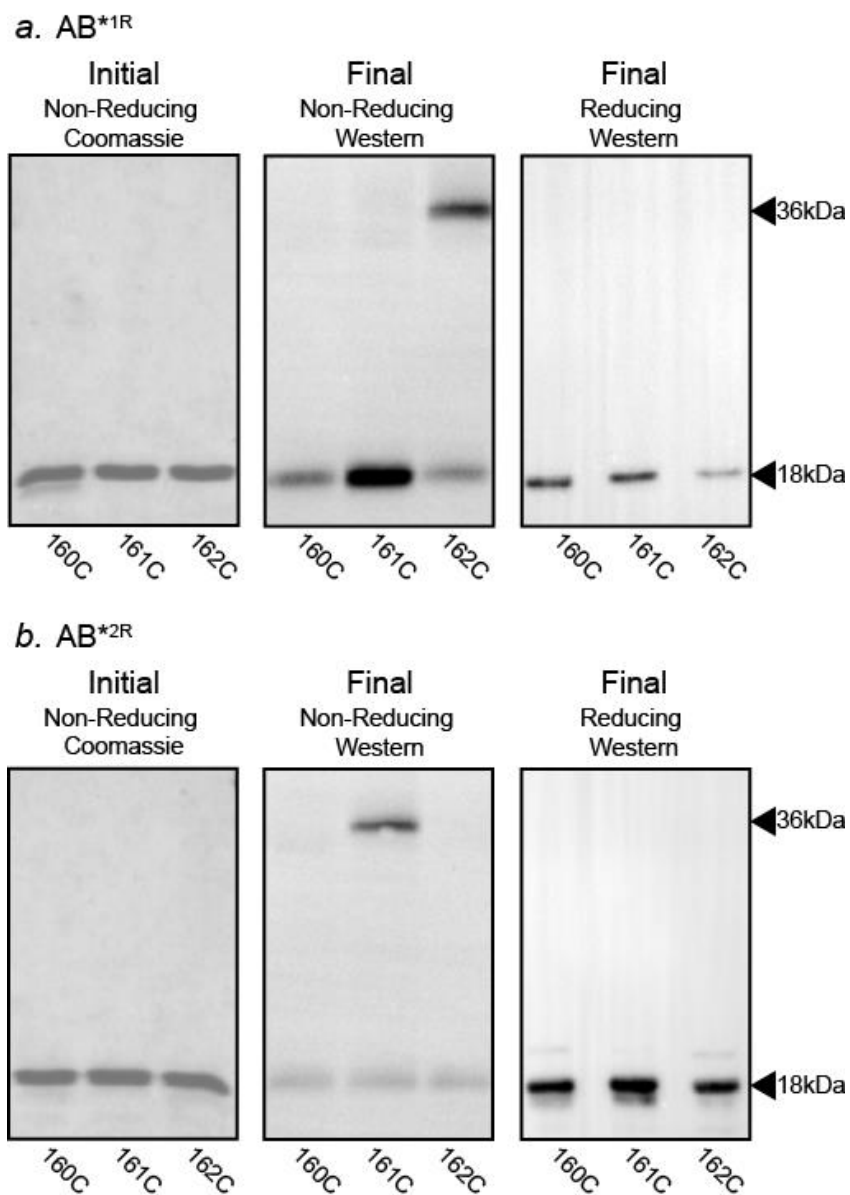
Figure 2.3. Idealized mutants are restricted to the intended register. Analysis of the formation of disulfides in A160C, L161C (register 2 probe), and E162C (register 1 probe) in (**a**) AB*^{1R} and (**b**) AB*^{2R}. (Left) Initial samples, which were heated and reduced, were visualized by Coomassie-stained, nonreducing SDS-PAGE. After cooling and dilution of the sample (without reducing agent), the formation of disulfides was assessed by nonreducing (Middle) and reducing (Right) SDS-PAGE, which were probed by western blot using anti-M1 polyclonal antibodies.

the idealizing mutations confined the B repeats to the intended registers and validate the use of cysteines as conformational probes.

Idealization of AB in register 1 had previously been shown to result in stabilization of the protein (McNamara et al., 2008). To assess whether this was the case for the idealization in register 2, the α-helical content of AB*^{2R}, as determined by circular dichroism (CD), was tracked with increasing temperature. At 4 °C the CD spectrum of AB*^{2R} was indistinguishable from those of the wild-type AB fragment (AB) and AB*^{1R} (Fig. 2.4a), indicating that the stabilizing mutations in register 2 had not changed the secondary structure of the molecule. Of particular note, AB*^{2R} maintained a much greater fraction of its α-helical content as compared to AB at temperatures greater than 20 °C (Fig. 2.4b). As shown previously, AB lost a substantial amount of its α-helical content with increasing temperature, whereas AB*^{2R} was more stable and behaved much like AB*^{1R}. Additionally, the melting profiles of AB*^{1R} and AB*^{2R} displayed cooperative transitions, whereas such transitions were not as evident for AB. Thus the idealization of the coiled coil in registers 1 or 2 yields molecules that are more stable than the wild-type molecule.

B REPEATS OF M1 PROTEIN EXIST IN MULTIPLE CONFORMATIONS

With the cysteine substitutions having been validated as conformational probes, we used these same substitutions to address the register of the B repeats in intact wild-type M1 protein. The same cysteine substitutions were introduced into wild-type M1 protein, and the procedure described above for assessing the formation of intra-dimer disulfide bonds was followed. Disulfide-linked dimers were evident for
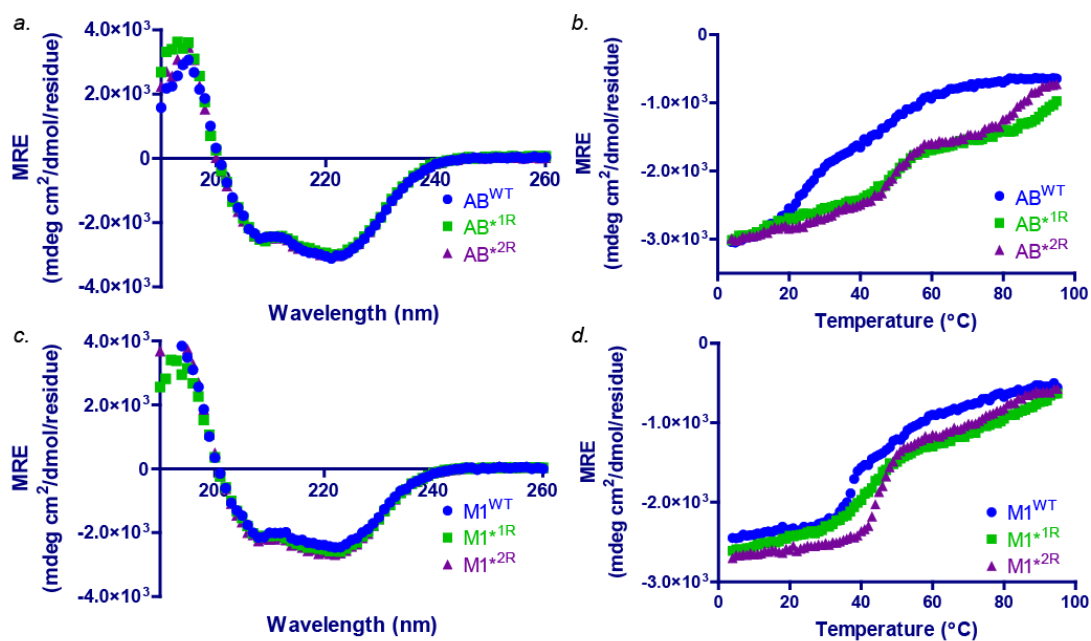
Figure 2.4. Idealized mutants are more stable than wild-type. Circular dichroism signal at 4 °C as a function of wavelength (**a** and **c**) and at 222 nm as a function of temperature (**b** and **d**) of AB constructs and intact M1 constructs. Wild-type is in blue, register 1 idealized in red, and register 2 idealized in green.
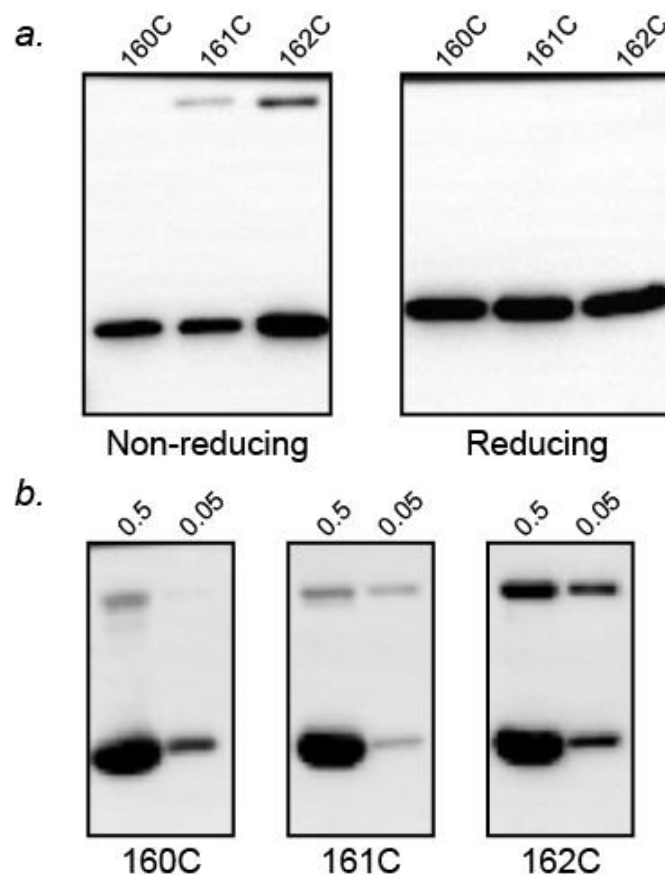
Figure 2.5. Wild-type M1 samples both register 1 and register 2. Analysis of intradimer disulfides in wt M1 protein using conformational probes A160C, L161C (register 2 probe), and E162C (register 1 probe). (a) After fully reducing the samples and removing the reducing agent through dilution the formation of disulfide linked dimers was visualized by non-reducing SDS-PAGE and probed for by an anti-His western. (b) To distinguish between intradimer and interdimer disulfide bonds, following reduction, proteins were incubated at a ten-fold higher concentration (mg/ml indicated above gel) where all mutants established disulfide linked dimers.

both the register 1 probe, E162C, and the register 2 probe, L161C, but not for the negative control, A160C (Fig. 2.5). To further demonstrate that the disulfide bonds observed in M1 L161C and E162C were intra-dimer and not inter-dimer, we carried out the same experiment with the M1 proteins at 10-fold higher concentration during the reassociation step (Fig. 2.5b). Under this condition, disulfide bonds were now evident for the negative control, L161C, indicating that the 10-fold higher M1 protein concentration during reassociation tended to lead to the formation of inter-dimer disulfides. Furthermore, this result demonstrates that the disulfides observed for the register 1 and 2 probes at the 10-fold lower reassociation concentration were indeed intra-dimer disulfides. Overall, this set of experiments provide evidence that the B repeats in the context of intact, wild-type M1 protein are flexible and dynamic, sampling both register 1 and register 2.

STABLE COILED COILS ARE NOT COMPETENT TO BIND FIBRINOGEN

We next sought to verify that AB*^{2R}, which is stabilized in the Fg-binding conformation, indeed binds Fg. To our surprise, we found that AB*^{2R} was deficient in Fg-binding. Its loss in interaction with Fg interaction was as great as that for AB*^{1R}, as assessed by a Ni^{2+}-NTA agarose co-precipitation experiment using His-tagged versions of the AB constructs and fibrinogen fragment D (FgD) (Fig. 2.6a). Although the CD results indicated that AB*^{2R} is a stable molecule, the deficiency in Fg-binding compelled us to examine its structure further. We collected HSQC NMR spectra for AB*^{2R} and AB (Fig. 2.7), and while the spectrum of AB showed broad peaks with
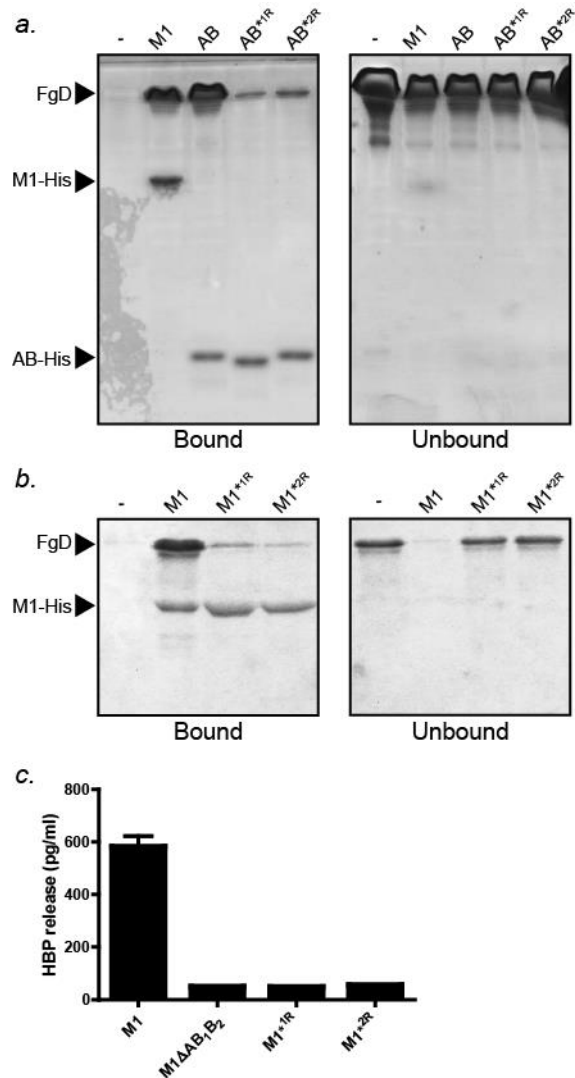
Figure 2.6. Register-idealized mutants are not competent to bind fibrinogen fragment D. Assay for fibrinogen binding of His-tagged AB fragments (a) and His-tagged M1 (b). Immobilized M1 constructs were incubated with FgD. Following washing and elution, bound FgD (left panel) and unbound FgD (right panel) was assessed through SDS-PAGE and stained with coomassie. As a negative control resin without protein was incubated with FgD (-). (c) *Ex vivo* functional result of diminished binding by register stabilized mutants. M proteins were incubated in whole blood and the ability to activate neutrophils was assayed for by HBP ELISA.

Figure 2.7. M1 AB*[2R] is a stable, structured protein. ^{1}H-^{15}N HSQC spectra of AB (a) and AB*[2R] (b) collected at 26 °C. The AB^{WT} spectrum has poor peak dispersion wi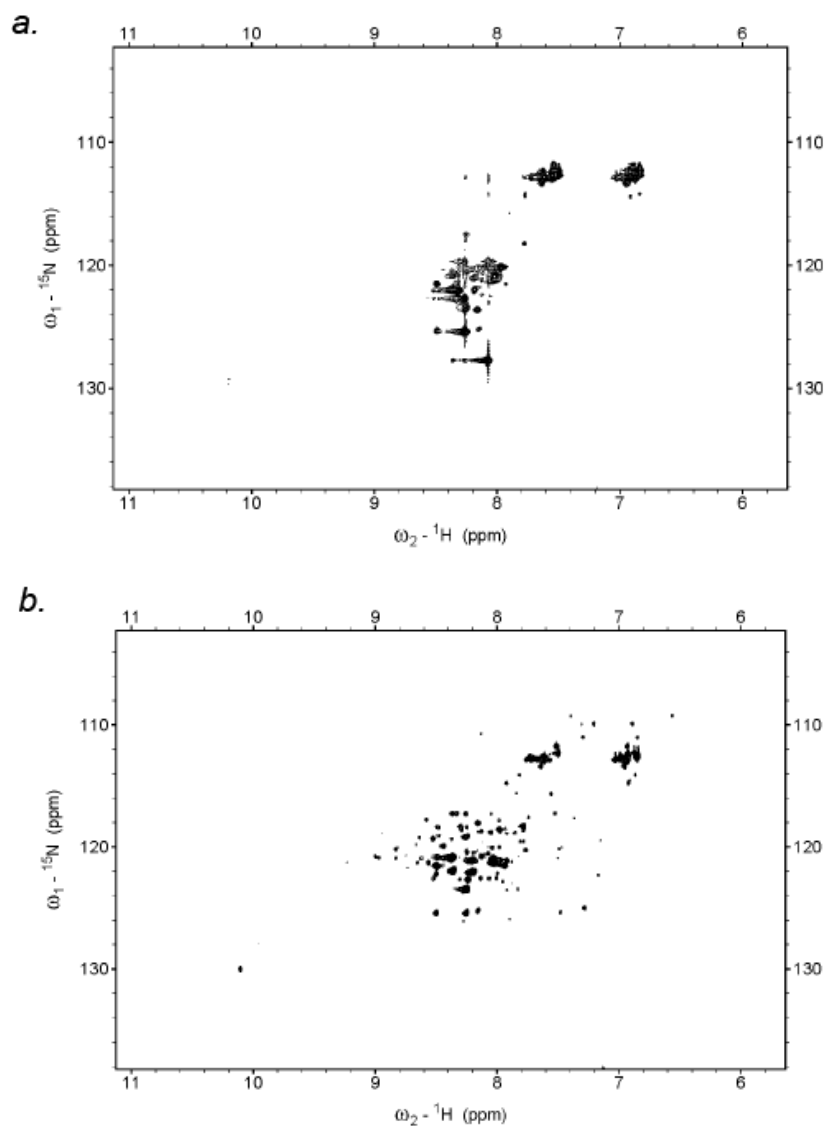th the NMR signal being confined to the random coil region (~7-9ppm). In contrast, the AB*[2R] spectrum has well dispersed and defined peaks.

very little dispersion, the spectrum of AB*^{2R} showed clear dispersion and distinct peaks. This NMR result provides further evidence that AB*^{2R} is a structurally stable protein, and suggests that the deficiency in Fg-binding is due to an increase in stability and concomitant loss of dynamics in the B repeats of M1 protein.

The results described above show a striking loss in Fg-binding due to idealization and concomitant stabilization of register 2 in the context of the AB fragment. This left open the possibility that these results were limited to the AB fragment and did not extend to intact M1 protein. To address this, we next asked what effects the idealization of register 2 has on intact M1 protein. Thermal melts of M1, M1*^{1R}, and M1*^{2R} reveal a pattern similar to that observed for the AB fragment, with the idealized mutants maintaining greater α-helical content at higher temperatures (Figs. 2.4c,d). M1*^{2R} appears to be the most stable of the three. Furthermore, co-precipitation experiments with His-tagged versions of the M1 constructs also revealed abrogated binding to FgD by M1*^{2R}, similar to the loss seen for M1*^{1R} (Fig. 2.6b). Intact M1 protein was too large to assess by NMR, and so we turned to a functional assay to ask whether the defect in M1*^{2R} was specific to Fg-binding or indicative of a nonspecific loss of native conformation. We assessed the ability of the M protein constructs to bind the Fc fragment of IgG. M1 protein binds the Fc fragment of IgG through an interaction downstream from the B repeats, in the S-C region. Both M1*^{2R} and M1*^{1R} maintained the ability to bind the Fc fragment (Fig. 2.8), indicating that the loss of Fg binding was specific. This result provides evidence that restricting the B repeats of M1 protein to a single register, although providing stability, diminishes the capacity to bind fibrinogen.
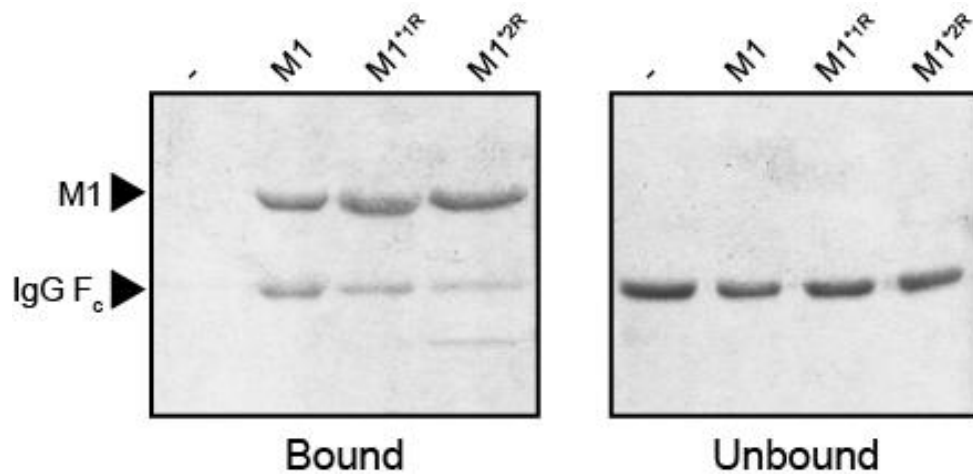
Figure 2.8. M1*^{1R} and M1*^{2R} retain the ability to bind IgG F$_c$. His-tagged M1 mutants were bound to Ni^{2+}-NTA resin and incubated with human IgG F$_c$. Unbound protein was collected and bound samples were washed and eluted with imidazole. Resin incubated with IgG F$_c$ was used as a negative control. Bound and unbound samples were resolved on a coomassie-stained SDS-PAGE gel. Register stabilized mutants show slight diminished binding.

As further verification of the loss of Fg binding, we examined a functional outcome of Fg binding by the M1 protein. That is the formation of a proinflammatory Fg-M1 supramolecular network, which elicits release of heparin binding protein (HBP) by human neutrophils (Macheboeuf et al., 2011). When wild-type M1 protein was added to whole human blood, HBP was found to be released, as previously reported (Fig. 2.6c). However, when M1*^{1R} or M1*^{2R} proteins were added to whole human blood, no released HBP was detected, consistent with the substantial decrease Fg binding in these register-idealized mutants.

SURFACE FIBRINOGEN BINDING ALSO DIMINISHED

While the experiments above indicate that register idealization results in a more stable form of soluble M1 protein, it remained possible that register idealization would not be tolerated when M1 protein is produced by GAS. To test this possibility, we expressed genes encoding M1*^{1R} and M1*^{2R} in *S. pyogenes* (*Δemm1*) (Lauth et al., 2009). The strains encoding these register-idealized variants expressed equivalent levels of surface-exposed M1 protein as the wild-type GAS 5448 strain, with these levels being determined by FACS analysis (Fig. 2.9a, Fig. 2.10a-e). As with soluble M1 protein, GAS surface-exposed M1*^{1R} and M1*^{2R} did not bind FgD, whereas wild-type M1, as expressed natively in GAS 5448 (carrying the empty pDCErm vector), or from plasmid pDCErm in *S. pyogenes* (*Δemm1*) bound FgD (Fig. 2.9c). Since intact Fg differs from FgD in being able to engage in avidity interactions with surface-exposed M1 protein, we examined Fg binding to GAS by FACS (Fig. 2.9b, Fig 2.10f-j). We found that GAS strains expressing M1*^{1R} or M1*^{2R} were greatly attenuated for
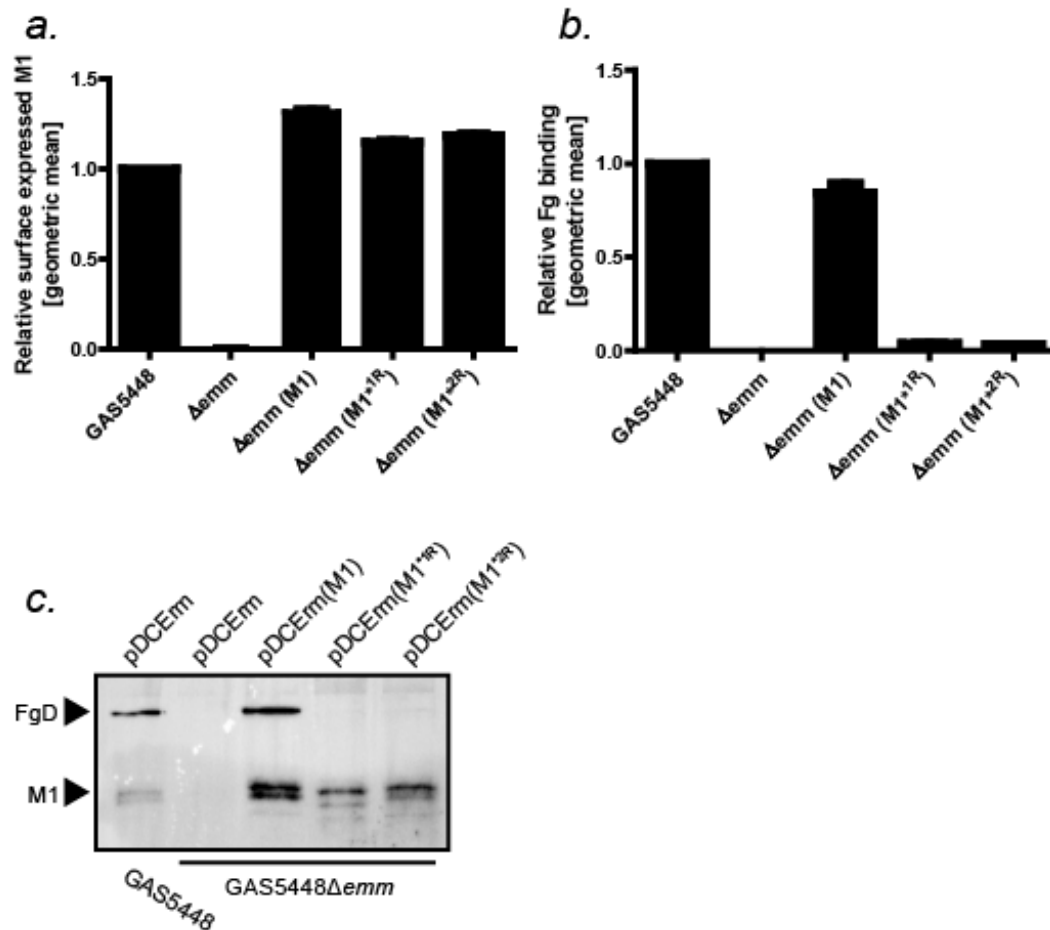
Figure 2.9. M1*^{1R} and M1*^{2R} are expressed on the GAS surface and not competent to bind fibrinogen. Surface expression of M1 constructs (a) and ability to bind FITC-labeled Fg (b) was assayed by FACS analysis and relative expression and binding compared to GAS 5448 is shown. (c) Complemented strains were incubated with FgD at 37 °C, washed and pelleted. Cell wall extracts were collected upon digestion with mutanolysin and ability to bind FgD was assayed by SDS-PAGE and western with an anti-M1 and anti-Fgγ probe, using GAS 5448 as a positive control.
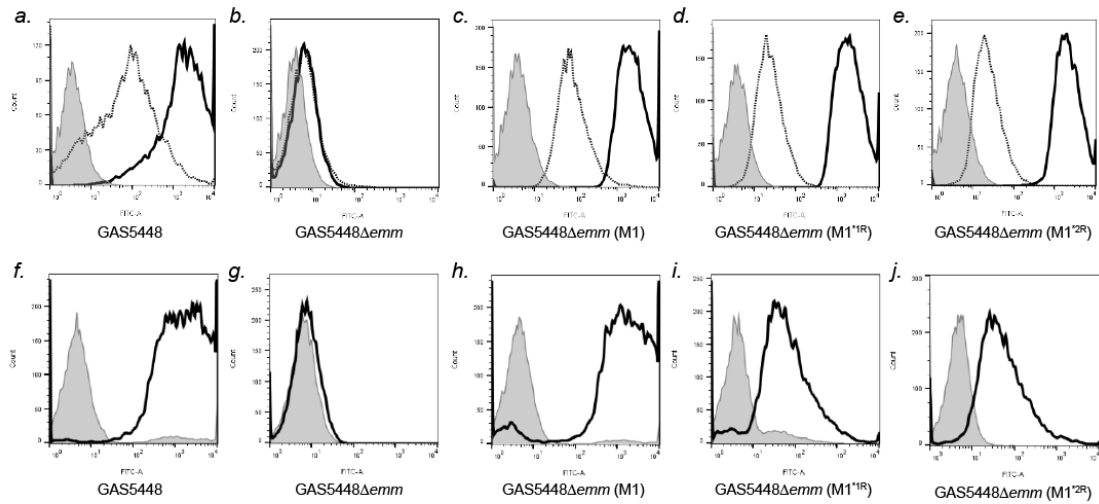
Figure 2.10. FACS histograms for surface expression of M1 and binding of fibrinogen. Histograms of surface M1 expression (a-e) and FITC-Fg binding (f-j). For surface M1 expression plotted is cells only (shaded grey), incubation with pre-imune sera and alexafluor-440 secondary (dotted), and incubation with anti-M1 sera and alexafluor-44 secondary (solid). For FITC-Fg binding plotted is cells only (shaded grey) and incubation with FITC-Fg (solid).

Fg binding compared to wild-type M1 protein, indicating that avidity is not able to

overcome the very weak interactions of the register-idealized mutants with Fg

DISCUSSION

Prior structural studies on M1 protein revealed a unique feature for a coiled

coil in that the coiled coil in the B repeats could exist in two conformations related by

a rotation of one helical face (Macheboeuf et al., 2011). These two conformations

arise from destabilizing amino acids in the dimer interface that favor the existence of

alternative conformations. Using disulfide probes, we confirmed that in solution the B

repeats are dynamic and the non-ideal properties of the B repeats lead M1 protein to

sample both conformations. While static crystallographic evidence indicates that the B

repeats adopt either register 1 or register 2, it is possible that hybrids or intermediates

of register 1 and 2 exist. Previous work revealed a decrease in the α-helical content of

M1 protein at physiological temperatures (Nilson et al., 1995). This phenomenon can

now be explained in part by the dynamics of the B repeats. Removal of the

destabilizing residues in the dimer interface of each register of the B repeats resulted

in an increase in the melting temperature indicating the destabilizing residues

contribute to dynamics in that region. While coiled coil structure is easily identified by

a heptad pattern in the amino acid sequence, specific variations in that pattern can

result in complex dynamics, thereby adding an additional level of intricacy to the

heptad pattern.

Dynamic motions of non-ideal coiled coils between multiple registers have previously been shown to be essential for function. In the HAMP domain of Af1503 from *Archaeoglobus fulgidus*, a conformational shift in registers of a tetrameric coiled coil is necessary to transmit signals across a membrane (Ferris et al., 2011; Hulko et al., 2006) and helix sliding in the coiled coil of dynein is required for communication between the ATPase and microtubule binding domain necessary for motor activity (Kon et al., 2009; Nishikawa et al., 2014). In both of these cases the coiled coil alternates between two conformations to transmit information about a binding event occurring at an attached domain. In this way, the flexibility of the coiled coil serves as a toggle indicating a signal is present or not. Similar to the two distinct dimeric coiled coil registers we see in M1, the coexistence of registers has been shown in the Nek2 leucine zipper where the rate of exchange between the registers allowed the simultaneous visualization of both conformations in a single NMR spectrum (Croasdale et al., 2011). Using cysteine substitutions to create stable disulfide-linked dimers, the authors gathered spectra on each individual register and confirmed the total signal from wild type Nek2 is a combination of signal from two dimeric coiled coil conformations. While a function is not known, it is surmised that the multiple conformations of the coiled coil of Nek2 is also used to transmit a signal.

However, in contrast to using the motion of the coiled coil to transmit a signal, M1 protein's use of dynamics in the coiled coil is unique. M1 protein samples from two registers, but there is also evidence for a splayed conformation, opening up the possibility for hybrids and intermediates between register 1 and register 2 as well. Flexibility of a non-ideal coiled coil has been observed in fragments of intermediate
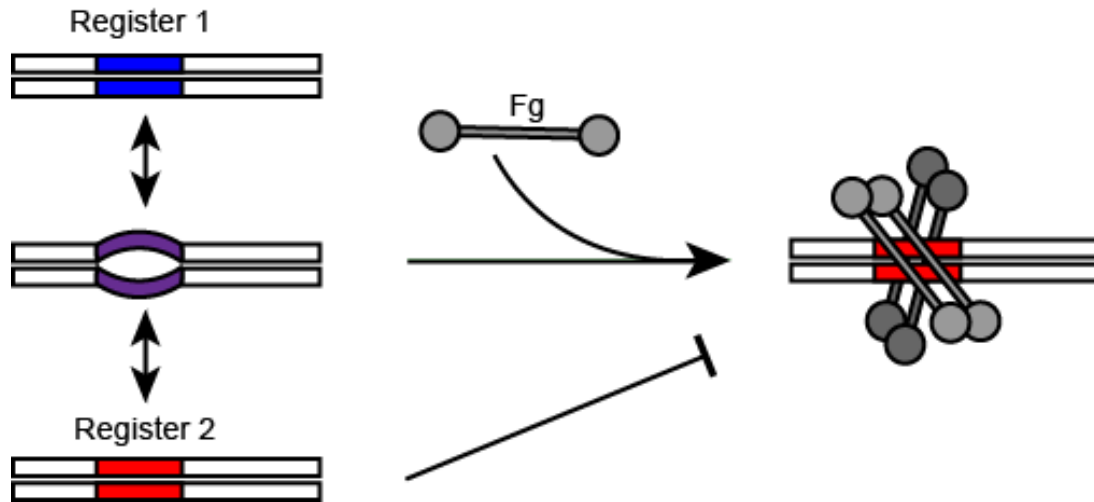
F**igure 2.11. Lure and catch model of M1-Fg interaction.** The B repeats of M1 protein are dynamic and in equilibrium between register 1 (blue), register 2 (red), and intermediate conformations (purple). An intermediate state attracts fibrinogen, after which the B repeats are locked into register 2. Stabilized register 2 is not able to recruit and bind fibrinogen.

filaments (Chernyatina et al., 2015) and modeled through molecular dynamics in cardiac myosin (Taylor et al., 2015). In both intermediate filaments and cardiac myosin, the instability of a dimeric coiled coil was shown to facilitate multimerization into larger helical bundles. In contrast, we show here that flexibility of the M1 coiled coil at the fibrinogen binding site is essential for binding in a non-coiled coil manner. In the M1-Fg model of binding, flexibility of the B repeats or an intermediate structure begins association with fibrinogen, and only after this initial contact is there a conformational shift that locks the B repeats into register 2 (Fig. 2.11). In this way, an intermediate structure "lures" fibrinogen and after that initial interaction, fibrinogen is "caught" when the B repeats lock into register 2.

Previously, the identification of an Fg-binding motif for M proteins has been elusive as the B repeats show little to no sequence conservation. This work presents an explanation for the great divergence of sequences and introduces another factor that would obscure the identification of a conserved sequence motif, the necessity for flexibility in the coiled coil. Fragment mapping in M5 protein implicates the B repeats as the Fg binding site (Ringdahl et al., 2000), yet there is little sequence similarity between M1 and M5 protein including the residues shown to interact with Fg in M1 protein. It was also observed that M1 and M5 bind fibrinogen non-competitively, further suggesting M1 and M5 do not bind fibrinogen identically. However, similar to M1 protein, the B repeats of M5 protein are also predicted to be a non-ideal coiled coil with multiple destabilizing residues in the putative dimer interface.

Chapter 2 in its entirety is pending publication as the Functional Significance for Coiled-coil Non-ideality in the Group A *Streptococcus* M1 Protein. Chelsea M. Stewart, Anna Henningham, Jason Cole, Andres Valderrama, Victor Nizet, Partho Ghosh. The dissertation author was the primary investigator and author of this work.

REFERENCES

Berge, Björck, 1995. Streptococcal cysteine proteinase releases biologically active fragments of streptococcal surface proteins. J. Biol. Chem. 270, 9862–7.

Chernyatina, A.A., Guzenko, D., Strelkov, S.V., 2015. Intermediate filament structure: the bottom-up approach. Curr. Opin. Cell Biol. 32, 65–72.

Cole, J.N., Barnett, T.C., Nizet, V., Walker, M.J., 2011. Molecular insight into invasive group A streptococcal disease. Nat. Rev. Microbiol. 9, 724–36.

Croasdale, R., Ivins, F., Muskett, F., Daviter, T., Scott, D., Hardy, T., Smerdon, S., Fry, A., Pfuhl, M., 2011. An Undecided Coiled Coil. The Journal of Biological Chemistry 286.

Cunningham, M.W., 2000. Pathogenesis of group A streptococcal infections. Clin. Microbiol. Rev. 13, 470–511.

Ferris, H.U., Dunin-Horkawicz, S., Mondéjar, L.G., Hulko, M., Hantke, K., Martin, J., Schultz, J.E., Zeth, K., Lupas, A.N., Coles, M., 2011. The mechanisms of HAMP-mediated signaling in transmembrane receptors. Structure 19, 378–85.

Fischetti, V.A., 1989. Streptococcal M protein: molecular design and biological behavior. Clin. Microbiol. Rev. 2, 285–314.

Herwald, H., Cramer, H., Mörgelin, M., Russell, W., Sollenberg, U., Norrby-Teglund, A., Flodgaard, H., Lindbom, L., Björck, L., 2004. M protein, a classical bacterial virulence determinant, forms complexes with fibrinogen that induce vascular leakage. Cell 116, 367–79.

Hirst, G.K., Lancefield, R.C., 1939. ANTIGENIC PROPERTIES OF THE TYPE-SPECIFIC SUBSTANCE DERIVED FROM GROUP A HEMOLYTIC STREPTOCOCCI. J. Exp. Med. 69, 425–45.

Hulko, M., Berndt, F., Gruber, M., Linder, J.U.U., Truffault, V., Schultz, A., Martin, J., Schultz, J.E., Lupas, A.N., Coles, M., 2006. The HAMP domain structure implies helix rotation in transmembrane signaling. Cell 126, 929–40.

Kon, T., Imamula, K., Roberts, A.J., Ohkura, R., Knight, P.J., Gibbons, I.R., Burgess, S.A., Sutoh, K., 2009. Helix sliding in the stalk coiled coil of dynein couples ATPase and microtubule binding. Nat. Struct. Mol. Biol. 16, 325–33.

Lauth, X., Köckritz-Blickwede, M. von, McNamara, C., Myskowski, S., Zinkernagel, A., Beall, B., Ghosh, P., Gallo, R., Nizet, V., 2009. M1 protein allows Group A streptococcal survival in phagocyte extracellular traps through cathelicidin inhibition. Journal of innate immunity 1, 202–14.

Lupas, A., Dyke, M. Van, Stock, J., 1991. Predicting coiled coils from protein sequences. Science 252, 1162–4.

Macheboeuf, P., Buffalo, C., Fu, C., Zinkernagel, A., Cole, J., Johnson, J., Nizet, V., Ghosh, P., 2011. Streptococcal M1 protein constructs a pathological host fibrinogen network. Nature 472, 64–8.

McNamara, C., Zinkernagel, A., Macheboeuf, P., Cunningham, M., Nizet, V., Ghosh, P., 2008. Coiled-coil irregularities and instabilities in group A Streptococcus M1 are required for virulence. Science (New York, N.Y.) 319, 1405–8.

Nilson, B., Frick, I.-M., Aakesson, P., Forsen, S., Bjoerck, L., Aakerstroem, B., Wikstroem, M., 1995. Structure and Stability of Protein H and the M1 Protein from Streptococcus pyogenes. Implications for Other Surface Proteins of Gram-Positive Bacteria. Biochemistry 34, 1368813698.

Nishikawa, Y., Oyama, T., Kamiya, N., Kon, T., Toyoshima, Y.Y., Nakamura, H., Kurisu, G., 2014. Structure of the entire stalk region of the Dynein motor domain. J. Mol. Biol. 426, 3232–45.

Phillips, G.N., Flicker, P.F., Cohen, C., Manjula, B.N., Fischetti, V.A., 1981. Streptococcal M protein: alpha-helical coiled-coil structure and arrangement on the cell surface. Proc. Natl. Acad. Sci. U.S.A. 78, 4689–93.

Ringdahl, U., Svensson, H.G., Kotarsky, H., Gustafsson, M., Weineisen, M., Sjöbring, U., 2000. A role for the fibrinogen-binding regions of streptococcal M proteins in phagocytosis resistance. Mol. Microbiol. 37, 1318–26.

Taylor, K.C., Buvoli, M., Korkmaz, E.N., Buvoli, A., Zheng, Y., Heinze, N.T., Cui, Q., Leinwand, L.A., Rayment, I., 2015. Skip residues modulate the structural properties of the myosin rod and guide thick filament assembly. Proc. Natl. Acad. Sci. U.S.A. 112, E3806–15.

Todd, E.W., Lancefield, R.C., 1928. VARIANTS OF HEMOLYTIC STREPTOCOCCI; THEIR RELATION TO TYPE-SPECIFIC SUBSTANCE, VIRULENCE, AND TOXIN. J. Exp. Med. 48, 751–67.

Tripet, B., Wagschal, K., Lavigne, P., Mant, C.T., Hodges, R.S., 2000. Effects of side-chain characteristics on stability and oligomerization state of a de novo-designed model coiled-coil: 20 amino acid substitutions in position "d". J. Mol. Biol. 300, 377–402.

Uchiyama, S., Andreoni, F., Zürcher, C., Schilcher, K., Ender, M., Madon, J., Matt, U., Ghosh, P., Nizet, V., Schuepbach, R., Zinkernagel, A., 2013. Coiled-coil irregularities of the M1 protein structure promote M1–fibrinogen interaction and influence group A Streptococcus host cell interactions and virulence. J. Mol. Med. 91, 861–9.

Wagschal, K., Tripet, B., Lavigne, P., Mant, C., Hodges, R.S., 1999. The role of position a in determining the stability and oligomerization state of alpha-helical coiled coils: 20 amino acid stability coefficients in the hydrophobic core of proteins. Protein Sci. 8, 2312–29.

Walker, M.J., Barnett, T.C., McArthur, J.D., Cole, J.N., Gillen, C.M., Henningham, A., Sriprakash, K.S., Sanderson-Smith, M.L., Nizet, V., 2014. Disease manifestations and pathogenic mechanisms of group a Streptococcus. Clin. Microbiol. Rev. 27, 264–301.

Woolfson, D.N., Alber, T., 1995. Predicting oligomerization states of coiled coils. Protein Sci. 4, 1596–607.

Chapter 3

Investigation into the Functional Role of

Each of the Fibrinogen Binding Sites of M1

Protein

INTRODUCTION

An integral aspect of infection is immune evasion, the ability of the pathogen to escape immune detection and elimination. *Streptococcus pyogenes*, also called group A *Streptococcus* (GAS), accomplishes this in part by coating itself with host proteins, preventing detection by antibodies (Sandin et al., 2006) and preventing deposition of complement (Chhatwal et al., 1986), thereby protecting GAS from phagocytosis. One such host protein is fibrinogen (Fg) which binds the antigenically variant M protein from GAS (KANTOR, 1965). Studies with M5 (Carlsson et al., 2005), M6 (Horstmann et al., 1992)**,** and M24 (Dale et al., 1996; Whitnack and Beachey, 1985) found that M protein was essential for preventing the deposition of complement in a fibrinogen-dependent manner and subsequent protection from phagocytosis.

While all M proteins are predicted to be α-helical parallel coiled coils, there is little sequence conservation among fibrinogen-binding M proteins. Structural studies on M1 protein identified three fibrinogen binding sites, one in the A region and one in each of the two B repeats (Macheboeuf et al., 2011). Each binding site of M1 protein can bind two molecules of Fg, thus the binding ratio is 2:6. The Fg-binding sites in M5 protein have been mapped to the B repeats, however they show little sequence homology to the B repeats of M1 (Ringdahl et al., 2000). Furthermore, M5 was shown to bind Fg non-competitively with M1 and is predicted to bind Fg in a 1:1 ratio. These differences raise the question of the Fg-binding requirements to confer

protection from phagocytosis; is a particular density of Fg required or a defined structural arrangement of Fg necessary?

To investigate the mechanism of Fg-dependent protection from phagocytosis, we used the M1-Fg system. Structural information from the co-crystal structure enabled the creation of mutants with each Fg-binding site deleted independently and in combination. Using a GAS (*Δemm1*) strain (Lauth et al., 2009), we complemented GAS (*Δemm1*) with our mutants M1ΔA, M1ΔB$_1$, M1ΔB$_2$, M1ΔB$_1$B$_2$, and M1ΔAB$_1$B$_2$ to investigate surface Fg binding and protection from phagocytosis (Fig. 3.1). In this way we will define the surface bound Fg requirement for immune evasion.

MATERIALS AND METHODS

COMPETENT *STREPTOCOCCUS PYOGENES*

A 5 mL culture of GAS was grown overnight in THB with 0.6% glycine (37 °C static culture). The overnight was diluted 1:10 in THB with 0.6% glycine and grown (37 °C static culture) until an OD$_{600}$ of 0.3. Bacteria were pelleted (3000 x *g*, 4°C, 5 min) and washed twice with 50 mL cold 0.625 M sucrose. Following the final wash, pelleted bacteria (3000 x *g*, 4 °C, 5 min) were resuspend in 250 µl cold 20% glucose (w/v), aliquoted into 50 µl aliquots, flash frozen, and stored at -80 °C.
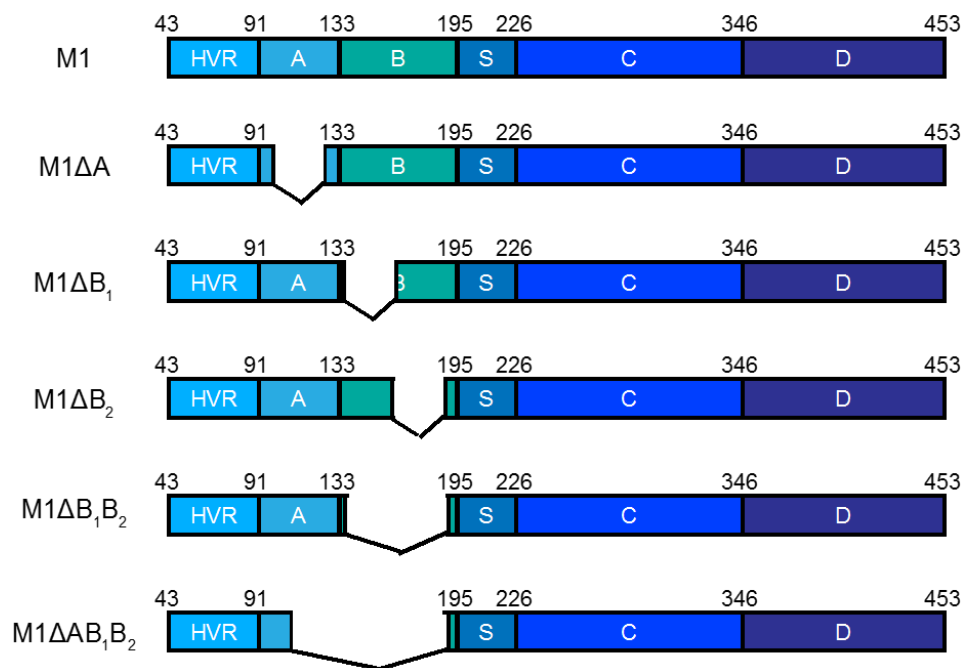
Figure 3.1 Schematic of Mature M1 Fibrinogen Binding Site Deletion Constructs. The three binding sites, one in the A region and one in each of the B repeats, were deleted independently and in combination.

CLONING AND DNA MANIPULATION

M1 deletion mutants on the pET28b plasmid as previously described (Macheboeuf et al., 2011) were cloned into pDCErm (M1) (Lauth et al., 2009) using sequence and ligation independent cloning (Li and Elledge, 2007). Deletions were as follows: M1ΔA (Δ98-125), M1ΔB$_1$ (Δ133-161), M1ΔB$_2$ (Δ162-189), M1ΔB$_1$B$_2$ (Δ134-189), and M1ΔAB$_1$B$_2$ (Δ105-189).

COMPLEMENTATION OF COMPETENT GAS

Deletion mutants in pDCErm were complemented back into a GAS5448 (*Δemm1*) strain (Lauth et al., 2009). Fifty ng plasmid was incubated with 50 µl competent GAS cell on ice for 30 minutes. Cells were transferred to a cold electroporation cuvette and shocked with 2.1 kV. Cells were recovered in 250 µl THB (37 °C, 1 h). Following recovery, transformants were selected for on THA with 5 µg/mL erythromycin. Successful transformation of the constructs was confirmed by PCR, after which strains were stored in 20% glycerol at -80 °C.

EXPRESSION IN COMPLEMENTED STRAINS

S. pyogenes was grown in stationary culture at 37 °C to mid-log phase and harvested by centrifugation (3000 x *g*, 15 min, 4 °C). Bacterial pellets were resuspended in PBS with 100 µg/ml purified FgD (Everse et al., 1995) and incubated with end-over-end rotation at 37 °C for 1 h. Bacteria were pelleted by centrifugation (3000 x *g*, 15 min, 4 °C), washed in 1 mL PBS three times, then resuspended in 40% sucrose, 100 mM KP$_i$, pH 6.2, 10 mM MgCl$_2$, 2 mg/mL lysozyme, 500 U/mL

mutanolysin, and incubated with rotation at 37 °C for 1 h. The soluble cell wall fraction was collected after centrifugation (13,000 x g, 10 min, RT) and resolved by SDS-PAGE. M1 protein was detected through Western blot. Samples were transferred from the polyacrylamide gel to a polyvinylidene fluoride membrane (Millipore) at 100 V for 40 min (wet transfer). Membranes were incubated in TBS (150 mM NaCl, 50 mM Tris, pH 8.0) for 10 min, and then blocked with 5% nonfat milk in TBS for 30 min. Membranes were incubated in TBS containing 5% nonfat milk, 0.05% Tween-20, and rabbit anti-M1 protein polyclonal antibody (1:500) at 4 °C overnight. Membranes were then washed three times in TBS containing 0.05% Tween-20 for 15 min each. Membranes were then incubated in TBS containing 5% nonfat milk, 0.05% Tween-20, and HRP-conjugated goat anti-rabbit IgG (1:5000, Santa Cruz Biotechnologies 2004) for 30 min at RT and washed as described above. SuperSignal West chemiluminescent substrate (Thermo Fisher Scientific) was used for detection, according to the manufacturer's instructions.

Bacterial surface expression of M protein was assayed through flow cytometry. For this, overnight growths of *S. pyogenes* were diluted into 10 mL THB and grown to mid-log phase. Cultures were pelleted by centrifugation (3000 x g, 10 min, 20 °C) and washed with 5 mL PBS containing 0.1% BSA. Bacteria were resuspended in PBS containing 0.1% BSA and incubated with either anti-M1 antibody or naïve serum (1:1000, 60 min, 4 °C). Bacteria were pelleted (3000 x g, 10 min, 20 °C) and washed twice with PBS containing 0.1% BSA. Samples were then incubated with the secondary antibody Alexa-488 anti-mouse IgG (1:500, 60 min, 4 °C, Life Technologies #A11001). Samples were pelleted by centrifugation (3000 x g, 10 min,

20 °C) and washed as above. Following the last wash, all samples were resuspended in PBS and analyzed by flow cytometry using a FACS Canto.

SURFACE FIBRINOGEN BINDING

Surface binding of Fg was assayed through flow cytometry. Fibrinogen was FITC labeled with the Fluoreporter kit (Life Technologies) according to the manufacturer's instructions. As above, overnight growths were diluted, grown to mid-log phase, washed with PBS containing 0.1% BSA and resuspended in RPMI with 0.2% BSA. To assay for Fg binding, bacteria were incubated with 50 μg/mL FITC-Fg for 1 h at 4 °C. Bacteria were pelleted (3000 x g, 5 min, 20 °C) and washed twice with PBS containing 0.1% BSA. Following the last wash, samples were resuspended in PBS containing 0.1% BSA and analyzed using a FACSCanto.

WHOLE BLOOD KILLING ASSAY

S. pyogenes was grown in stationary culture at 37 °C to mid-log phase and harvested by centrifugation (3000 x g, 15 min, 4 °C). Bacteria were washed in PBS and resuspended in PBS to 2 x 10^5 cells/mL. Two hundred μL of cells were incubated with 800 μL whole blood freshly collected from healthy donors at 37 °C with end over end rotation. Time points were collected at 0, 1, 2, 3, and 4 h. Briefly, 10 μL was collected and serially diluted 1:10. Dilutions were plated on THA plates, incubated overnight at 37 °C, and colony forming units (CFU) were counted to determine percent survival.

THP-1 KILLING ASSAY

THP-1 cells were plated in a 96-well plate at 2 x 10^4 cells/mL and differentiated into macrophages by incubation with 200 nM PMA in RPMI at 37 °C for 72 h. One hour prior to infection, media containing PMA was removed and replaced with pre-warmed RPMI. *S. pyogenes* was grown in stationary culture at 37 °C to mid-log phase and harvested by centrifugation (3000 x *g*, 15 min, 4 °C). Bacteria were washed in PBS and resuspended in PBS, and added to cells at an MOI of 1 in 5% human serum. Cells were incubated with bacteria for 2 h at 37 °C, following which the wells were triterated with PBS containing 0.25% Triton-X100. Bacteria was serially diluted and plated on THA. Following overnight growth at 37 °C, colonies were counted and percent survival was determined. Antibody against group A carbohydrate was added during infection at either a 1:1000 or 1:5000 dilution.

RESULTS

COMPLEMENTED STRAINS EXPRESS DELETION MUTANTS ON THE SURFACE

To investigate the role of the multiplicity of Fg binding sites in M1 protein, we individually deleted the three Fg-binding sites in M1 protein and complemented a GAS *emm1* knockout with the M1 deletion mutants. To verify surface expression of the constructs, we used flow cytometry with a polyclonal antibody directed against wild type M1 protein (Fig. 3.2b). As expected, wild type GAS expressed M1 protein and GAS (*Δemm1*) did not. The complemented strains showed varying levels of

surface anti-M1 binding, either due to differing expression levels or differing affinities of the polyclonal antibodies. To verify that the surface-expressed M1 protein is the desired deletion mutant, cell wall extracts were prepared and separated by denaturing SDS-PAGE (Fig. 3.2c). M1 protein was visualized by an anti-M1 western, which confirmed the predicted molecular weight of M1 protein in the constructs containing deletions. Thus our complemented strains express the desired construct on the surface.

FIBRINOGEN BINDING SITE DELETIONS DIMINISH THE ABILITY TO BIND FIBRINOGEN

To verify that deleting the fibrinogen binding sites in M1 protein reduced or eliminated the ability of GAS to bind Fg, we incubated the deletion strains with FgD and pelleted the bacteria to collect unbound FgD and surface-associated FgD. To reduce background binding, the bacterial pellets were washed in PBS and cell wall extracts were collected. The extracts were separated on a denaturing SDS-PAGE and M1 and FgD were detected by Western blot (Fig. 3.3a). As expected wild type GAS and intact M1-complemented GAS (*Δemm1*) showed strong binding to FgD, while GAS (*Δemm1*) containing pDCErm showed only background binding. Interestingly, GAS (*Δemm1*) expressing M1ΔA, M1ΔB$_1$, M1ΔB$_2$, or M1ΔB$_1$B$_2$ maintained substantial binding to FgD. Only GAS (*Δemm1*) expressing M1ΔAB$_1$B$_2$ showed a drastic decrease in FgD binding.
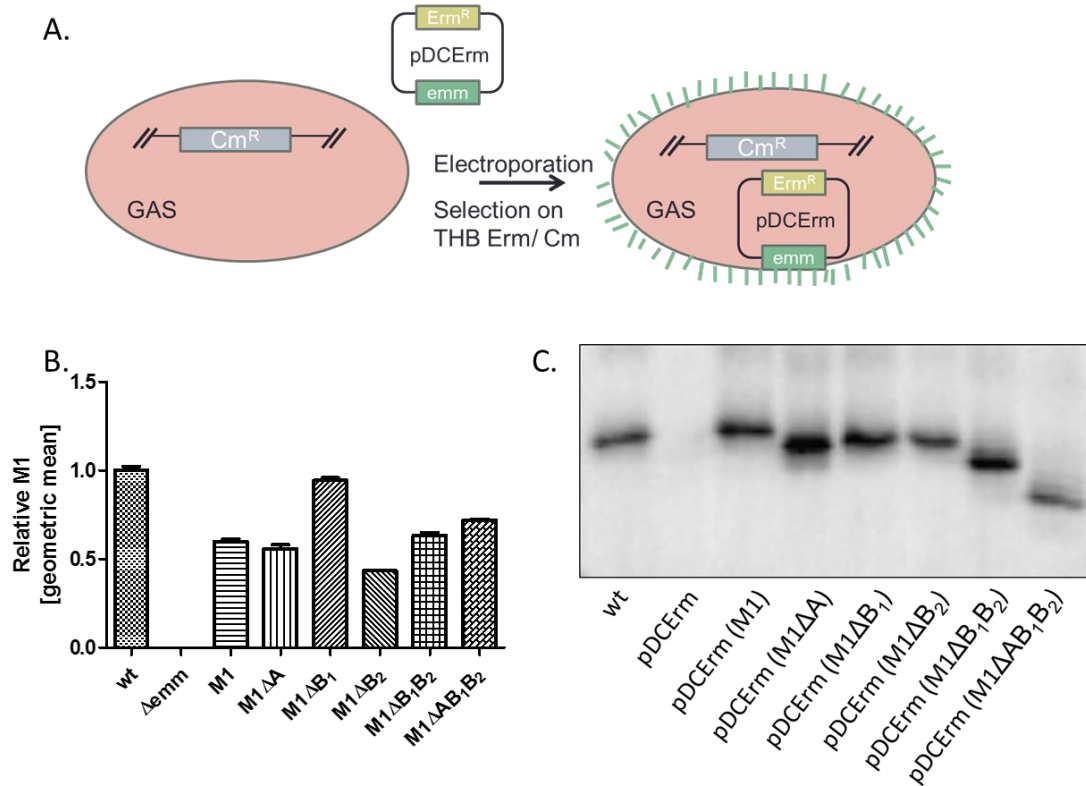
Figure 3.2. Complementation of GASΔ*emm1* with M1 constructs. (A) Model of complementation strategy. We complemented GAS (*Δemm1*) with pDCErm containing each M1 construct. Successful transformants were selected for with erythromycin. (B) Surface expression of the constructs was confirmed through anti-M1 FACS. Given is the relative level of M1 to wt GAS. (C) Western blot of cell wall extracts of complemented GAS (*Δemm1*) showing a decrease in molecular weight as more binding sites are deleted.

We next asked whether this phenomenon is true for intact Fg as well. Intact Fg has multiple M1 binding sites, so can engage in avidity interactions. We used FITC-labeled Fg to probe for surface association of Fg through flow cytometry (Fig 3.3b). As expected, wild type GAS bound high levels of Fg, while GAS (*Δemm1*) did not. Complementing GAS (*Δemm1*) with intact M1 restored most of the binding, and individually deletioning the Fg-bindings sites resulted in diminishing Fg binding. Interestingly, the strain expressing M1ΔAB$_1$B$_2$, presumably lacking all Fg binding sites, still retained 28% of wild-type levels of bound Fg. In contrast, GAS (*Δemm1*) showed under 1% binding suggesting there is another region of M1 or another surface factor that can interact with Fg or interacts with FgD weakly then binds Fg with avidity.

WHOLE BLOOD SURVIVAL

Surface-expressed M1 protein can recruit host fibrinogen to coat the bacteria with host proteins to help evade immune detection and elimination. It has previously been shown that survival in whole blood is dependent on M1 expression (Ringdahl et al., 2000), specifically the B repeats. We sought to further define the fibrinogen-binding requirements for protection from phagocytosis to provide a mechanistic role for the multiplicity of Fg binding sites of M1 protein. To do so, we attempted to establish a whole blood survival assay using our deletion mutant strains. The strains are grown to mid-log phase, washed and added to freshly drawn blood from a health donor. By nature of the assay, each experiment is run with blood from a single donor each time. As a result, the assay results showed donor dependence. While one donor
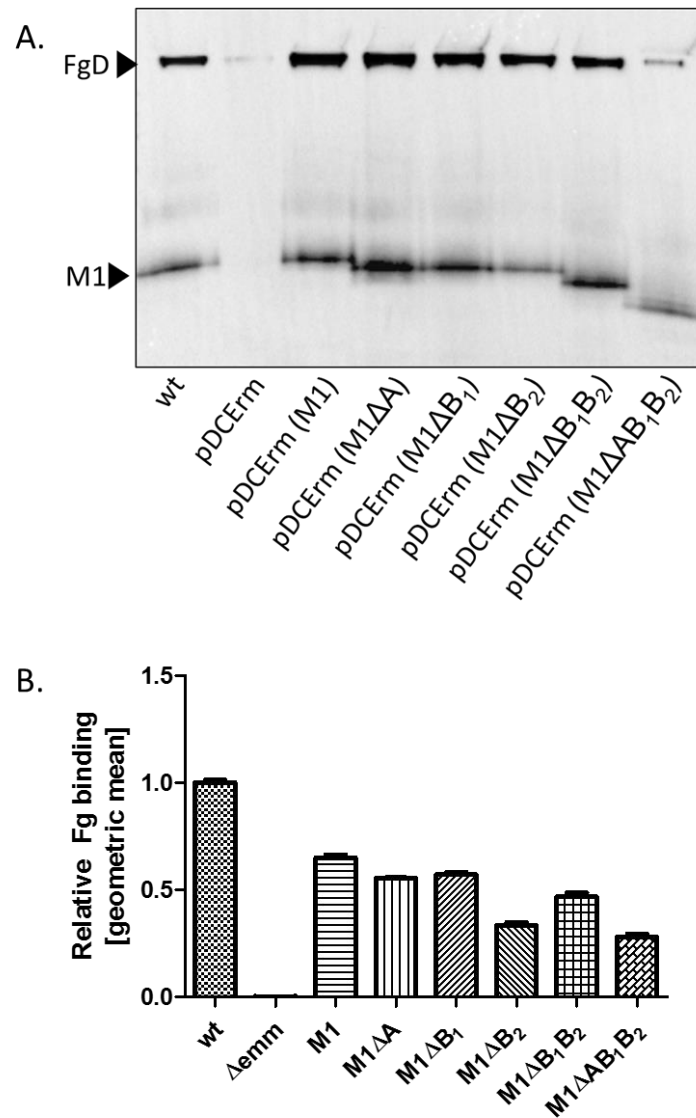
Figure 3.3 Surface Fibrinogen Binding. (A) Complemented strains were incubated with FgD at 37 °C, washed and pelleted. Cell wall extracts were collected upon digestion with mutanolysin and ability to bind FgD was assayed by SDS-PAGE and western with an anti-M1 and anti-Fgγ probe, using GAS 5448 as a positive control. (B) Surface Fg binding was assayed by flow cytometry and showed a decrease in binding with removal of Fg binding sites. Given is level of Fg binding relative to wt GAS.

may show M1 protein-dependent survival, in whose blood GAS shows high survival in contrast to the efficient killing of GAS (*Δemm1*), another donor shows no difference between GAS (*Δemm1*) and wild type GAS survival (Fig 3.4). Furthermore, repeating the experiment with blood from the same donor on different days showed inconsistent levels of killing, indicating there are additional variables in blood that cannot currently be controlled for and whole blood survival is not a robust method to assay for phagocytosis protection.

CULTURED MACROPHAGE PHAGOCYTOSIS

As the whole blood assays showed donor dependence, we turned to assaying phagocytosis using cultured macrophages. THP-1 cells are monocytes that differentiate into macrophages following incubation with PMA. Bacteria were grown to mid-log phase, preincubated with Fg or not, and added to THP-1 cells at an MOI of 1 in the presence of 5% human serum as a source of complement. Bacterial survival was enumerated after 2 hours by triterating the cells and plating for CFU (Fig. 3.5a). While wild type GAS showed survival and growth, GAS (*Δemm1*) were killed by the THP-1 cells. However, complementing GAS (*Δemm1*) with intact M1 did not recover the ability to survive. Furthermore, there was no change in survival after pre-incubation with Fg and the survival of GAS (*Δemm1*) complemented with $M1\Delta AB_1B_2$ was equivalent to that of GAS (*Δemm1*) complemented with intact M1.

Phagocytosis can also occur as a result of surface bound opsonizing antibodies. Through coating the bacterial surface with Fg, GAS could prevent the binding of antibodies as well as C3, further protecting from opsonophagocytosis. We next
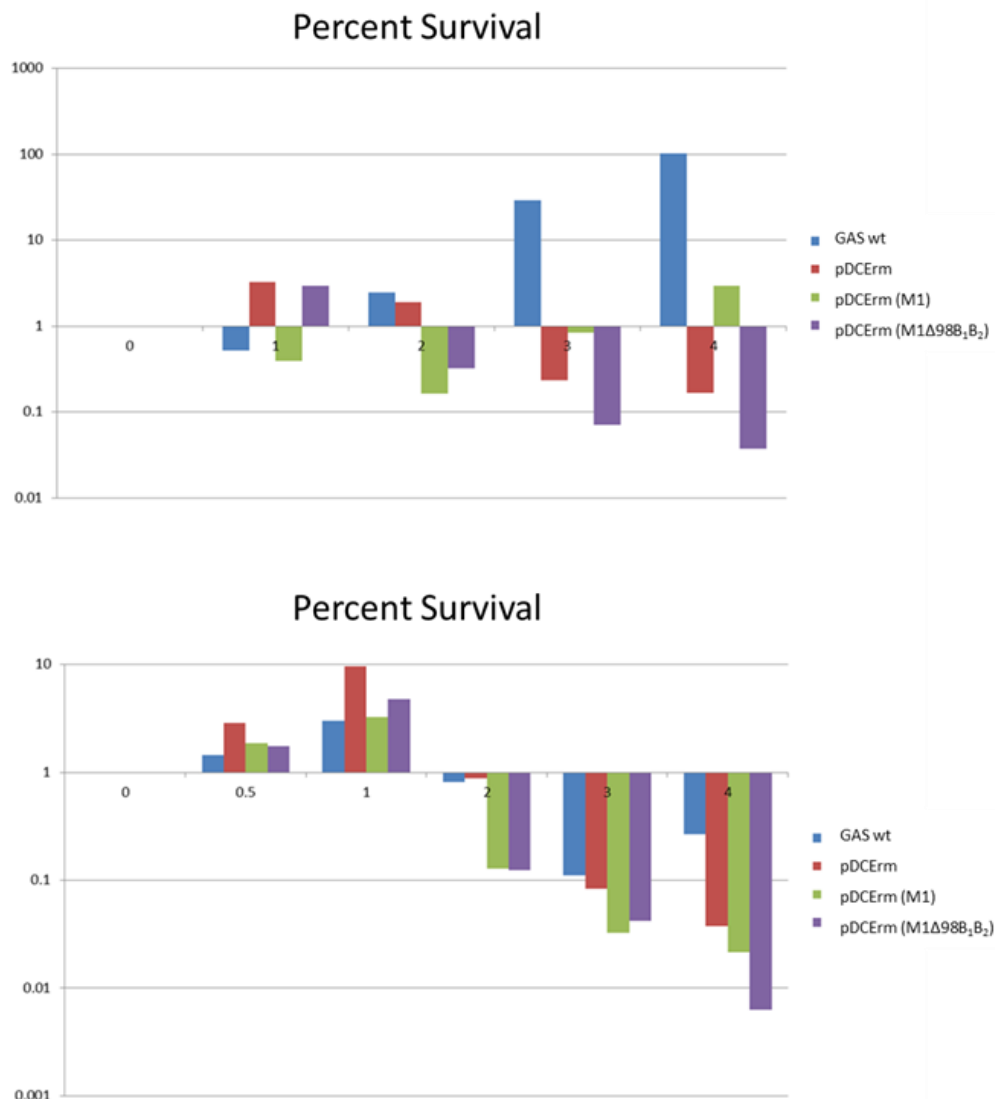
Figure 3.4. Donor Dependency of GAS Survival in Whole Blood. GAS was incubated in freshly collect blood from a healthy donor of the day of the experiment. Hour time points were collected and percent survival was determined. The axis is one hundred percent, growth is indicated above the axis and death is indicated below the axis. In donor 1 (top) there is a M1-dependent survival, while in donor 2 (bottom) there is no difference. Data is representative of n=6 experiments.

infected THP-1 cells with GAS either pretreated with Fg or not in the presence of 5% serum and IgG against group A carbohydrate (Fig. 3.5b-c). However, there was no difference between survival in the presence of antibody or not. In both cases, GAS (*Δemm1*) showed a slight decrease in survival compared to wt GAS. However complementation of GAS (*Δemm1*) with either M1 or M1ΔAB$_1$B$_2$ showed equivalent levels of survival as GAS (*Δemm1*). This work with THP-1 cells indicates that plasmid complementation does not restore a wild type phenotype. While there is surface expression from the introduced plasmid, that level of expression may be variable or plasmid expression may impact other bacterial pathways.

DISCUSSION

The surface-expressed M1 protein contributes to pathogenesis in part through its interaction with fibrinogen. When released from the bacterial cell surface by bacterial and neutrophil proteases, M1 protein and Fg form a supramolecular complex required for activating neutrophils (Macheboeuf et al., 2011). This network is formed from two sequential Fg binding sites in the B repeats that create a crosshatched arrangement of M1 and Fg. Interestingly there is an additional Fg binding site in the A region of M1 protein whose role in unknown. This work sought to address the function of the multiplicity of Fg binding sites in protecting GAS from phagocytosis. To address the role of each Fg binding site we created deletions in M1 protein at each of the Fg binding sites individually and in combination and complemented
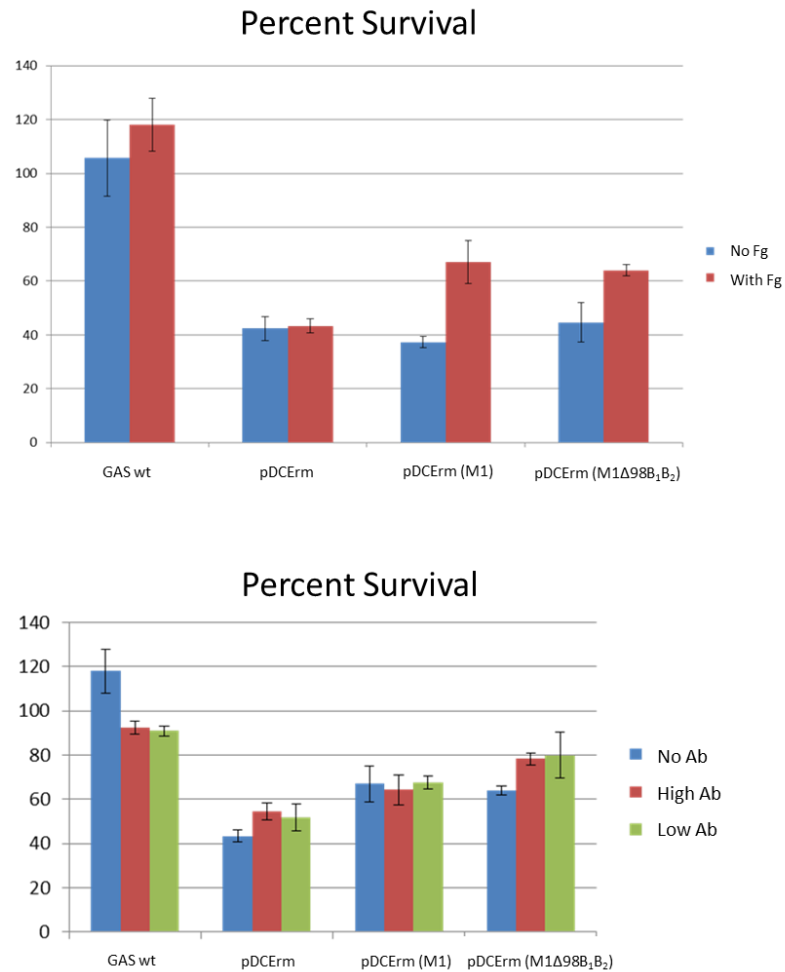
Figure 3.5. THP-1 Killing Assay. (A) GAS was incubated with differentiated THP-1 cells for 2 h after pre-incubation with Fg or not. While there is a decrease in survival in GAS (Δ*emm1*), complementation with intact M1 does not restore survival. Nor is there a difference between incubation with Fg or not. (B) The addition of an IgG against group A carbohydrate during incubation had no influence on survival either.

GAS (*Δemm1*) with these deletion constructs. We verified surface expression of the constructs and confirmed the deletions led to a decrease in surface-bound Fg.

With these strains as probes for the functional role of each Fg site, we attempted to establish an assay for phagocytosis. Previous work used whole blood survival to address this question, however our results varied donor to donor and day to day. The donor dependence of whole blood survival has been previously noted (Husmann et al., 1995; Kotarsky et al., 2000; Ringdahl et al., 2000; Thern et al., 1998). Donor dependence has also been noted for immune activation. Kahn et al. began investigating the reason behind this variation and found donors to be grouped into responders and non-responders to GAS infection (Kahn et al., 2008). It was found that anti-M1 IgG was crucial in determining whether the donor's immune cells would be activated by M1 GAS or not. While that work was done looking at immune activation rather than phagocytosis resistance, immune activation contributes to the ability of bacteria to survive in whole blood. Thus as an added control for future whole blood experiments, it would be prudent to titre anti-M antibody levels in conjunction with assaying for survival.

Next we turned to cultured macrophages to assay for phagocytosis. After 2 hrs of infection, wild type GAS survived while GAS (Δ*emm1*) was killed. However complementation with intact M1 did not restore wild type levels of survival, and complementation with M1ΔAB$_1$B$_2$ showed an equivalent low level of survival. The inability of complemented strains to show a survival phenotype was seen in prior work as well. Kotarsky et al., complemented GAS (Δ*emm5*) with a plasmid encoding M22 protein and complemented GAS (Δ*emm22*) with a plasmid encoding M5 protein

(Kotarsky et al., 2000). While these strains expressed the desired M protein on the surface, survival in whole blood was not restored. A similar experiment was done with M4 and M6 (Husmann et al., 1995) with the same result. These results in conjunction with the data presented here would indicate that the plasmid complementation system is not equivalent to the chromosomal reincorporation. While the construct on the plasmid is expressed on the surface, additional genetic changes could occur that influence the survival phenotype of GAS. In contrast, Carlsson et al. successfully showed Fg-dependent prevention of complement deposition using a chromosomal mutants (Carlsson et al., 2005). To address the function of the fibrinogen binding sites, rather than using complemented strains, the binding site deletions should be made within the bacterial genome.

REFERENCES

Carlsson, F., Sandin, C., Lindahl, G., 2005. Human fibrinogen bound to Streptococcus pyogenes M protein inhibits complement deposition via the classical pathway. Mol. Microbiol. 56, 28–39.

Chhatwal, G.S., Dutra, I.S., Blobel, H., 1986. Specific binding sites for monomeric and aggregated beta 2-microglobulin on surface of groups A, B, C, and G streptococci. Microbiol. Immunol. 30, 155–64.

Dale, J.B., Washburn, R.G., Marques, M.B., Wessels, M.R., 1996. Hyaluronate capsule and surface M protein in resistance to opsonization of group A streptococci. Infect. Immun. 64, 1495–501.

Everse, S.J., Pelletier, H., Doolittle, R.F., 1995. Crystallization of fragment D from human fibrinogen. Protein Sci. 4, 1013–6.

Horstmann, R.D., Sievertsen, H.J., Leippe, M., Fischetti, V.A., 1992. Role of fibrinogen in complement inhibition by streptococcal M protein. Infect. Immun. 60, 5036–41.

Husmann, L.K., Scott, J.R., Lindahl, G., Stenberg, L., 1995. Expression of the Arp protein, a member of the M protein family, is not sufficient to inhibit phagocytosis of Streptococcus pyogenes. Infect. Immun. 63, 345–8.

Kahn, F., Mörgelin, M., Shannon, O., Norrby-Teglund, A., Herwald, H., Olin, A., Björck, L., 2008. Antibodies against a Surface Protein of Streptococcus pyogenes Promote a Pathological Inflammatory Response. PLoS Pathog 4, e1000149.

KANTOR, F.S., 1965. FIBROGEN PRECIPITATION BY STREPTOCOCCAL M PROTEIN. II. RENAL LESIONS INDUCED BY INTRAVENOUS INJECTION OF M PROTEIN INTO MICE AND RATS. J. Exp. Med. 121, 861–72.

Kotarsky, H., Thern, A., Lindahl, G., Sjöbring, U., 2000. Strain-specific restriction of the antiphagocytic property of group A streptococcal M proteins. Infect. Immun. 68, 107–12.

Lauth, X., Köckritz-Blickwede, M. von, McNamara, C., Myskowski, S., Zinkernagel, A., Beall, B., Ghosh, P., Gallo, R., Nizet, V., 2009. M1 protein allows Group A streptococcal survival in phagocyte extracellular traps through cathelicidin inhibition. Journal of innate immunity 1, 202–14.

Li, M.Z., Elledge, S.J., 2007. Harnessing homologous recombination in vitro to generate recombinant DNA via SLIC. Nat. Methods 4, 251–6.

Macheboeuf, P., Buffalo, C., Fu, C., Zinkernagel, A., Cole, J., Johnson, J., Nizet, V., Ghosh, P., 2011. Streptococcal M1 protein constructs a pathological host fibrinogen network. Nature 472, 64–8.

Ringdahl, U., Svensson, H.G., Kotarsky, H., Gustafsson, M., Weineisen, M., Sjöbring, U., 2000. A role for the fibrinogen-binding regions of streptococcal M proteins in phagocytosis resistance. Mol. Microbiol. 37, 1318–26.

Sandin, C., Carlsson, F., Lindahl, G., 2006. Binding of human plasma proteins to Streptococcus pyogenes M protein determines the location of opsonic and non-opsonic epitopes. Mol. Microbiol. 59, 20–30.

Thern, A., Wästfelt, M., Lindahl, G., 1998. Expression of two different antiphagocytic M proteins by Streptococcus pyogenes of the OF+ lineage. J. Immunol. 160, 860–9.

Whitnack, E., Beachey, E.H., 1985. Inhibition of complement-mediated opsonization and phagocytosis of Streptococcus pyogenes by D fragments of fibrinogen and fibrin bound to cell surface M protein. J. Exp. Med. 162, 1983–97.

Chapter 4

Conclusions

Crystallographic studies revealed unique features of the fibrinogen binding sites of M1 protein (McNamara 2009, Macheboeuf 2011). M1 protein is a non-ideal coiled coil, and the fibrinogen binding sites were found to exist in two conformations, or registers, related by one turn of the helix. Additionally, two fibrinogen binding sites were identified in the B repeats, one in each repeat, as well as one additional site in the A region. The work presented here sought to address the functional roles of the dual registers and of the multiplicity of binding sites. This understanding contributes to knowledge of the mechanism of immune recognition and of GAS pathogenesis.

STRUCTURAL DYNAMICS

In Chapter 2 the role of the non-ideal coiled coil was investigated. It was shown that wild type M protein is dynamic at the B repeats and samples from at least two distinct conformations. It was also shown that the flexibility that arose from disruptive residues at the dimer interface of the coiled coil at the fibrinogen binding sites is required for fibrinogen binding.

Future work will seek to further describe the dynamics at the B repeats. NMR studies are being done to try to visualize the dynamics in solution. Through a collaboration with the Pfuhl lab at King's College, we hope to capture the AB fragment of M1 protein in each or any of the conformations it may adopt, similar to the work Croasdale has done on Nek2. Additionally, we can develop hypotheses for the scope of dynamics through computational biology and molecular dynamics. Beginning with the determined crystal structure in register 2, we can remove fibrinogen and observe the motions available to the BC fragment of M1 protein.

Combining these strategies we will develop a deeper understanding of the dynamics of the non-ideal coiled coil M1. This knowledge will help develop a broader understanding of the nature of coiled coils and the nuances to the heptad pattern that could lead to unique conformations and functions.

MULTIPLICITY OF BINDING SITES

In Chapter 3 the function of each fibrinogen binding site was studied. By complementing GAS ($\Delta emm1$) with pDCErm containing M1 with deletions in one or multiple fibrinogen binding sites, I created strains of GAS capable of recruiting different levels of fibrinogen to its surface. I verified the strains expressed the desired construct on its surface and that there was diminished fibrinogen binding. Interestingly, the strain expressing M1ΔAB$_1$B$_2$, a deletion in all identified fibrinogen binding sites, retained a substantial amount of bound fibrinogen. This could have been due to avidity from intact fibrinogen, but is a phenomenon to be investigated further.

Another interesting phenomenon is the inability of complementation with intact M1 to recover a wild type phenotype. Thus rather than complementation, future studies should use chromosomal integration of mutations to address the question of protection from phagocytosis. Additional studies will look at levels of complement deposition in relation to surface fibrinogen levels, to identify if binding levels are correlated or if there is a point of saturation. Once the relationship between surface fibrinogen binding and C3 deposition is defined, electron microscopy will be used to describe the structural mechanism behind the prevention of C3 deposition.

The goal of these future work is to further our understanding of the unique structural features of the M1-Fg interaction and M1 protein itself. Understanding of the M1-Fg interaction and its contribution to pathogenesis can then be applied to and investigated in other Fg-binding M proteins. This knowledge can be used to develop novel therapeutics and guide vaccine development. This work will also contribute to our knowledge of coiled coils and help define additional structural features that contribute to protein function.